Published in : Chemical Engineering Journal (2025), vol.516, pp. 1–15
DOI: 10.1016/j.cej.2025.163998
Status : Postprint (Author's version)

FOAM-TO-ADHESIVE RECYCLING OF SELF-BLOWN NON-ISOCYANATE POLYURETHANE FOAMS FACILITATED BY INTEGRATION OF DISULFIDE EXCHANGEABLE BONDS AND MOISTURE

Víctor D. Lechuga-Islas [a,c], Emeline Gillissen [a,c], Maxime Bourguignon [a], Bruno Grignard [a,b,*], Christophe Detrembleur [a,c,*]

[a] *Center for Education and Research on Macromolecules (CERM), CESAM Research Unit, University of Liege, Sart-Tilman B6 a, 4000 Liege, Belgium*
[b] *FRITCO2T Platform, University of Liege, Sart-Tilman B6a, 4000 Liege, Belgium*
[c] *WEL Research Institute, Avenue Pasteur, 6, 1300 Wavre, Belgium*
**Corresponding authors at: Center for Education and Research on Macromolecules (CERM), CESAM Research Unit, University of Liege, Sart-Tilman B6 a, 4000 Liege, Belgium*

Abstract

Non-isocyanate polyurethane foams (NIPUFs) offer a safer, more sustainable alternative to conventional isocyanate-based foams. However, polyhydroxyurethane-type NIPUFs, despite containing covalent adaptable bonds, require harsh reprocessing conditions (160–170 °C for several hours), which limits practical recyclability due to unwanted side reactions. In this work, we introduce cystamine-based dynamic disulfide bonds into self-blown NIPUFs, enabling effective reprocessing at significantly milder conditions (as low as 90 °C) without requiring catalysts or generating any side reactions. Critically, the combination of dynamic disulfide chemistry with NIPU hydroplasticization synergistically enhances bond exchange dynamics, accelerating the foam-to-film transformation under gentle, cost-efficient conditions. This powerful strategy allows the resulting films to be repurposed into high-performance adhesives, showing lap-shear strengths comparable to cyanoacrylate thermoset formulations on stainless steel and glass–steel interfaces, and exceeding those of tested commercial polyurethane thermoset and hot-melt adhesives. Notably, the adhesives also demonstrate strong adhesion, in the same range as benchmarks, on glass and nylon fabrics. Furthermore, the cystamine-containing NIPU adhesives exhibit fast, heat-triggered debonding and are reusable across multiple cycles without notable performance loss. This study presents a versatile and scalable approach to NIPUF design, where the synergistic effect of hydroplasticization and dynamic disulfide bonds enables facile, efficient recycling and repurposing into adhesives—broadening application potential and extending material lifespan.

Keywords : Non-isocyanate polyurethanes, Foams, Covalent adaptable networks, Adhesives, Moisture, Recycling

1. Introduction

Polyurethanes (PU) are among the most employed polymers in the market due to their outstanding properties and manufacture possibilities. Polyurethane foams (PUFs) lead the worldwide foam market, accounting for 65 % of total PU-based materials consumption. This application is followed by the production of PU-based coatings (13 %), elastomers (12 %), and adhesives (7 %) [1,2]. Many commercial PUFs are produced through water-induced self-blowing of polyol and harmful di- or polyisocyanate formulations, which creates crosslinked networks with fixed topology [3,4]. Due to the variety of formulations, the obtained PUFs have found numerous applications in materials engineering from comfort (matrasses, footwear, seats, etc.) to thermal and sound insulation, filtration systems, reinforced composites, personal protective equipment etc., [5,6]. However, although the crosslinked network structure of the foam provides chemical resistance, durability and excellent mechanical properties, these predominantly fossil-based materials are non-processable, non-biodegradable, and inevitably generate waste once used or damaged.

In this context, addressing the end-of-life of PUFs has become a priority to comply with regulation changes. Besides incineration for energy recovery or mechanical and chemical recycling, recent methodologies exploit the dissociative carbamate exchange reactions of urethane linkages to reprocess ground thermoset PUFs into value-added second-life materials (*e.g.*, adhesives, coatings, or composites) [7–12]. Although convenient, this approach usually requires temperatures above 140 °C, high loading forces, and long periods of time to reshape the PUFs [13]. Such harsh conditions can also have effects on the chemical composition of the reprocessed materials, which in turn modifies their appearance and thermomechanical properties.

To accelerate carbamate exchange and ameliorate the PUFs reprocessing, some strategies have implemented catalysts, such as dibutyltin dilaurate [9], triazabicyclodecene [14], zirconium(IV) acetylacetonate [$Zr(acac)_4$] or zirconium tetrakis(2,2,6,6-tetramethyl-3,5- heptanedionate) [$Zr(tmhd)_4$] [10,15]. The latter however may reduce the process efficiency as the catalysts remain in the recycled material which in turn poses potential toxicity concerns after use and disposal [2]. Another strategy to accelerate and facilitate PUFs repurposing under milder conditions is to introduce a second type of reversible or exchangeable bonds with increased dynamicity within the network, such as oxime-carbamate [16,17], β-amino ester [18], TAD-indole [19] or disulfide groups [20,21]. While disulfide chemistry is particularly attractive due to their relatively accessible introduction to foam or film PU materials [22–24], current approaches still depend on toxic isocyanates and require elevated temperatures and long reprocessing times.

Aiming to create greener alternatives to produce foam materials, non-isocyanate polyurethane foams (NIPUFs) have emerged as potential alternatives to tackle both the environmental concerns and the difficulty to reprocess PUFs. NIPUFs are mainly composed of poly(hydroxyurethane) (PHU) crosslinked networks, produced through the aminolysis of poly(five-membered cyclic carbonate)s with polyamines. Foaming is achieved either through addition of external blowing agents [25–27] or via *in situ* reactions, producing so-called self-blown foams [28–35]. Recently, we have introduced several self-blowing foaming processes by exploiting the ambivalent reactivity of cyclic carbonate groups to construct the PHU network while simultaneously promoting partial decarboxylation to generate CO_2 as blowing agent [33,34,36]. By exploiting this approach and implementing reactive formulations (such as cascade exothermic reactions) [34–38], we achieved self-blown NIPUFs at temperatures ranging from 120 °C to room temperature, with blowing times as short as a few minutes [33–39]. These robust

and up-scalable strategies are potentially compatible with existing foaming infrastructures, remove the need for external blowing agents, and can be adapted to a variety of starting materials (e.g., biobased multifunctional cyclic carbonates [32,40–43], functionalized polyamines [44], or (bio) fillers) [26,45]. In comparison with common PUFs, NIPUFs reprocessing capabilities are facilitated due to the presence of additional hydroxyl groups along the polymer structure, which promotes dynamic exchange reactions through associative transcarbamoylation mechanisms and reversible urethane linkage formation, even under catalyst-free conditions [31,46,47]. Hence, compression molding of NIPUFs into films has been reported to occur in a range of temperature from 140–160 °C and loading pressures of 7–10 Tons for 1–3 h [31,32,36,45,47–49]. As a proof of concept, NIPUFs have been readily repurposed into films as structural composites by hot pressing onto nylon fabric [36]. However, these reprocessing conditions did not avoid side reactions, such as urea formation, which limited multiple recycling cycles [35].

Introducing additional exchangeable bonds into NIPUFs is expected to further facilitate their reprocessing, minimizing risks of deterioration during recycling, a common challenge in PU materials [19,20]. While NIPU networks with dual dynamic features have shown recyclability benefits [50–53], examples related to NIPUFs are scarce. For instance, by designing PHU networks with additional in-chain ester linkages, Torkelson et al. [41] capitalized on transesterification reactions to reshape the NIPUFs into elastomers at 150 °C, for 1 h under 7 Tons pressure. Recently, they also developed non-isocyanate polythiourethane (NIPTU) foams capable of auto-oxidation to produce disulfide bonds endowing the foams with exchangeable sulfide chemistry [40]. This development utilized surfactants and external blowing agents to produce foams with microcellular structure, which allowed reprocessability through injection, extrusion and compression molding (140 –180 $^{\circ}C$, 1 Ton, for 3 –5 min).

To overcome the harsh reprocessing conditions typically associated with NIPUFs, herein, we present a simple and unprecedentedly fast foam-to-film strategy based on dual dynamic linkages in self-blown NIPUFs. Specifically, we incorporated cystamine, a renewable disulfide diamine derived from cystine decarboxylation [54], into a water- induced self-blowing NIPU system. The introduction of dynamic disulfide groups is compatible with foam formation and enables a rapid, catalyst-free foam-to-film reprocessing under milder conditions than conventional PHU-based exchange mechanisms. Remarkably, we exploit foam hydroplasticization, typically considered a drawback in NIPUFs, as an efficient, cost-effective tool to accelerate bond exchange dynamics, working synergistically with the dynamic network to further accelerate reprocessing. We exploit this facilitated reprocessing features to transform the foams into high-performance adhesives for stainless steel, glass, and nylon fibers substrates. Unlike thermosetting adhesives, the foam-to-adhesive strategy offers thermoset adhesives featured by on- demand and repeatable bonding/debonding ability without performance loss, while providing creep resistance, ductility, and recyclability.

2. Experimental section

2.1. MATERIALS

Ethylene carbonate (98 %, EC), Hexamethylenediamine (98 %, HMDA), and 1,8-Diazabicyclo[5.4.0]undec-7-ene (98 %, DBU) were purchased from Sigma Aldrich. Cystamine

dihydrochloride (98 %) was purchased from abcr GmbH. Trimethylolpropane triglycidyl carbonate (TMPTC) was synthesized from CO_2 and trimethylolpropane triglycidyl ether as reported by our group [55]. HMDA was distilled prior use. All other reagents and solvents were used without any further purification. Benchmark adhesives Bison PU MAX (PU prepolymer base), Bison Textile (Natural rubber (NR) base), Loctite Super Glue (Ethyl cyanoacrylate (ECA) base), and Rapid Universal hot melt adhesive ((HM) Ethylene Vinyl Acetate copolymer and resin base) were purchased from Brico (Belgium) and used according to the recommendations of the manufacturer (see description below).

Stainless steel substrates (AK Steel, 10 × 50 mm × 0.5 mm thickness) were kindly provided by the Mechanical Department of the University of Liege. Micro glass slides (26 × 76 mm × 1 mm thickness) were obtained from Knittel glass. Nylon fabric Cordura (texturized polyamide 185 g m^{-2}, 330 density) was acquired from Extremtextil (Germany). Before use, the substrates were cleaned with an acetone/isopropanol (1/1, v/v) mixture to remove any unwanted weak boundary layers, such as surface contaminants, oil, grease, oxides, etc. Stainless-steel and glass slides were additionally washed with water and wiped with tissue paper. This procedure was repeated 3 times. Each substrate was dried at 50 °C for at least 4 h. Additional tests were conducted using stainless-steel substrates with an added sanding pre-treatment (120 grit sandpaper) before bonding. The adhesive joints used to determine tensile lap-shear strength were prepared as follows:

NIPU film: A dried piece of NIPU film (0.65 mm thick, ~0.12 g) was deposited onto a substrate covering the gluing area (~100 mm^2 for stainless steel and stainless steel-glass and ~200 mm^2 for glass joints). Next, a second substrate was placed in contact, and the joint was assembled using a hot press (CARVER, Model 4122) for the indicated loading force, time, and temperature. After that, the adhesively bonded joints were allowed to cool down on metal plates at room temperature for 30 min before lap-shear measurements. In the case of nylon fiber joints, a piece of NIPU film (0.65 mm thick) was welded onto a freshly cleaned nylon fabric (120 °C, 2 Tons, 30 min). The obtained composite was then cut into strips (1.0 × 30 cm), and pairs of strips were welded again (120 °C, 2 Tons, 30 min) with an overlap area of ~100 mm^2 for lap-shear measurements.

Benchmarks: PU adhesive (~0.7 g) was applied thinly and evenly to a substrate using a spreader. Then a second substrate was joined to cover a gluing area of ~100 mm^2. The assembly was pressed for at least 4 h under a loading force of 2 kg cm^{-2}. NR adhesive (~0.1 g) was thinly and evenly applied to cover the indicated bonding area. After a 5-minute rest, the joint was assembled by pressing the substrates together. ECA adhesive (~0.5 g) was evenly distributed on one substrate to cover the indicated bonding area. The joint was immediately assembled by pressing an additional substrate together for at least 30 s until the bond set. The assembly was left undisturbed for at least 30 min. HM adhesive sticks were heated in a glue gun for 5 min. Once melted, the adhesive was dispensed (~0.6 g) to cover the indicated bonding area of the substrate. Then, the joint was quickly assembled as the adhesive cooled and set within seconds. The assembly was left undisturbed to cure for at least 30 min.

2.2. SYNTHETIC PROCEDURES

2.2.1. CYSTAMINE SYNTHESIS

Cystamine dihydrochloride (8.05 g, 35.7 mmol) was dissolved in distilled water (200 mL) at T = 15 °C. Then, potassium hydroxide (6.1 g, 108.7 mmol) was slowly added under vigorous stirring to avoid raising the temperature of the solution. The mixture was then stirred for 15 min at T < 20 °C. The

resulting mixture was extracted with 4 × 150 ml CH_2Cl_2, and the organic phase was dried over $MgSO_4$ and filtered. After solvent evaporation under vacuum at room temperature, a slightly yellow oil was recovered (4.25 g, 79 %). Characterization data matched previously reported literature [56]: ^{1}H NMR (400 MHz, $CDCl_3$) δ (ppm) 1.31 (br, 4H), 2.73 (t, 4H), 2.98 (t, 4H). ^{13}C NMR (400 MHz, $CDCl_3$) δ (ppm) 42.59, 40.62. The final product was stored at − 20 °C to avoid decomposition.

2.2.2. MODEL REACTIONS

Aminolysis and hydrolysis of EC in presence of cystamine was examined by the following standard procedure: EC (0.40 g, 4.54 mmol, pre-heated at 40 °C) and cystamine (0.345 g, 2.26 mmol), were mixed in a flame-dried reaction tube provided with a magnetic stirrer. After adding DBU (0.034 g, 0.223 mmol), the tube was sealed and placed in a pre-heated oil bath at the desired temperature under continuous stirring. Samples were taken from the mixture periodically. Each sample was directly solubilized and quenched in a solution of 600 μL of DMSO-d_6 containing 50 μL of formic acid for their analysis by ^{1}H NMR spectroscopy. At each time, the EC hydrolysis was measured by the formula: *EC hydrolysis* = $\frac{I_b}{I_a+I_b}$, where I_a is the intensity of signal at 4.2 ppm related to EC and I_b is the intensity of signal at 3.3 ppm related to ethylene glycol (obtained by hydrolysis of EC, Fig. S1). Model reactions were conducted according to this procedure at different temperatures (i. e., 100, 50 and 25 °C, Fig. 1).

2.2.3. FOAMING PROCESS

TMPTC and cystamine or HMDA (Tables S1 and S2) were mixed in a square silicon mold (A = 16 cm^2) until a viscous mixture was obtained. Next, water and DBU were added and mixed at room temperature for 1 min until a homogeneous mixture was obtained. The resulting mixture was placed in a pre-heated oven at 100 °C for 3 h. The foam was then cooled to room temperature before demolding and drying at 80 °C for 24 h in a vacuum oven. To minimize ambient moisture effects, foams were stored in a sealed desiccator under vacuum.

2.2.4. FOAM REPROCESSING

Dried foams were frozen in liquid N_2 and then ground into a fine powder using an IKA A11 basic grinder. Next, the powdered material was evenly spread between two nylon and two aluminum plates within a square aluminum mold (thickness = 0.65 mm). This assembly was hot- pressed under the indicated loading force, time, and temperature. After 5–10 min of pressing, the pressure was briefly released and re-applied three times to remove any air bubbles and allow the formation of homogeneous films. The obtained polymer film was removed from the mold, and specimens were cut for characterization or use as adhesives. Reprocessing of moistened foam samples was performed using ground foams that had been previously equilibrated at room temperature and 80 % relative humidity (RH) for 72 h.

2.3. CHARACTERIZATION METHODS

^{1}H, ^{13}C, and DOSY Nuclear Magnetic Resonance (NMR) spectroscopy experiments were performed on a Bruker Avance 400 MHz spectrometer at 25 °C in the Fourier transform mode.

Fourier Transform Infrared (FT-IR) spectroscopy characterizations were performed on a Nicolet iS5 FT-IR spectrometer from ThermoFisher Scientific, equipped with a diamond attenuated transmission reflectance (ATR) device. Sample spectra were recorded in 16 scans, over the range of 4000 to 500 cm^{-1} with a nominal resolution of 4 cm^{-1}.

Humidity-dependent experiments were conducted on samples conditioned in a Weisstechnik CareEvent climate chamber at controlled RH levels (40–80 %) and room temperature for at least 24 h. Scanning electron microscopy (SEM) images were obtained with a FEI QUANTA 600 microscope. The cells size distributions were estimated by the mean diameter measurements of at least 100 cells using ImageJ software.

Differential scanning calorimetry (DSC) was performed on a DSC250 calorimeter from TA Instruments. The samples were analyzed in hermetic aluminum pans. Glass transition temperature (T_g) was estimated after drying the foam or film in vacuum at 80 °C for 8 h. Then, each sample was conditioned by a first ramp from room temperature to 120 °C with 5 min of equilibration in the DSC apparatus. Then, T_g was measured for three cycles more at a heating rate of 10 °C min^{-1} over a temperature range from − 50 to 120 °C. T_g of dried samples was determined from the third cycle. The T_g of moistened samples was measured during the first DSC heating cycle without prior conditioning step.

Thermogravimetric analysis (TGA) was performed on a TGA2 instrument from Mettler Toledo. Around 10 mg of sample were heated at 10 °C min^{-1} until 600 °C under a nitrogen atmosphere (50 mL min^{-1}). $T_{d5\ \%}$ was measured as the temperature at 5 % mass loss from mass at 100 °C. Water uptake (%) of moistened samples was estimated based on the initial weight loss observed below 150 °C, which was attributed to water desorption and moisture content.

Compression tests were performed on an INSTRON 5594 equipped with a 10,000 N load cell device in compression mode. Compression was performed at a rate of 2 mm min^{-1} on cubic foam samples of ~1 cm^3. Compression tests were also performed on foam cubes equilibrated at 40 and 80 % RH for 24 h. Dimensional stability was assessed by comparing sample volume before and after humidity equilibration.

Gel content (GC) was estimated by weighing a cubic sample (~1 cm^3) of each foam before (m_1) and after immersion in THF. After 24 h, the solvent was removed, and the foam was dried at room temperature for at least 48 h and under vacuum for 16 h more at 50 °C (m_2). GC was calculated by the formula: $GC = \frac{m_2}{m_1} \times 100\ \%$. The average density (D) of the foams was obtained by weighing three foamed cubic samples of known dimensions, according to the formula $D = \frac{m}{V}$

Stress-relaxation, shear creep, and creep-recovery experiments were conducted on a Rheometer ARES-G2 from TA Instruments using circular film samples (8 mm diameter × 0.65 mm thickness). Each stress relaxation experiment consisted of a first dry-conditioning step at 80 °C for 1 h, followed by an equilibration step at the desired temperature for 10 min. Stress-relaxation measurements were performed with an axial force of 1 N (sensitivity of 0.05 N) in compression to initialize the experiment at the set conditions of temperature with a sustained strain of 1 % and a measurement of the decrease of the sample's stress over time. All series of stress relaxation experiments at varying temperatures were conducted sequentially on the same sample, beginning with the highest indicated temperature. Stress relaxation of moistened samples was measured (without dry-conditioning step) using film samples that had been previously equilibrated at 60–80 % RH. Shear creep and creep-recovery tests were conducted within the linear viscoelastic regime for equilibrated samples at 50 °C for 10 min prior measurement. Then, a constant shear stress (σ) of 3 kPa was applied for 30,000 s, followed by a 7200-second recovery period under zero stress. To capture pure creep and exclude initial delayed elastic deformation, creep strain values ($\Delta\varepsilon$) were estimated as the difference in strain between t = 30,000 s and t = 1800 s.

Lap-shear strength (LSS) and uniaxial creep tests were performed using an Instron 5594 equipped with a 10,000 N load cell and a temperature-controlled chamber. Uniaxial creep tests were performed by recording the strain of bonded stainless-steel joints under a fixed tensile force and temperature. LSS tests were performed by applying force parallel to the adhesive bond with a displacement rate of 2 mm min^{-1} until pulling apart the bonded joints. The gripping length on both sides of test specimens was 25 mm. The LSS was calculated by the formula: $\tau_{lap}=\frac{P}{A}$, where τ_{lap} is LSS (in N mm^{-2} or MPa), *P* is the maximum loading force to remove and break the adhesive (in N), and *A* is the overlapped gluing area of the adhesive joint. The tests were performed on at least 4 repeated samples for each type of adhesive to report the average LSS and standard deviation. After testing, adhesive recycling was performed by scraping the adhesive off the debonded substrate facilitated by elevated temperature (heating gun ~100 °C). The recovered adhesive was then reformed in a mold (120 °C, 2 Tons, 30 min), cut into square pieces and welded onto fresh substrates (at the indicated welding conditions), covering the previously indicated bonding area. The same procedure was repeated for each subsequent recycling cycle.

3. Results and discussion

We selected here the simplest and cheapest system for producing reprocessable NIPUFs, i.e., the water-induced self-blowing procedure (Scheme 1A). This process involves catalyzing the partial hydrolysis of the cyclic carbonate (5CC) monomer to release CO_2 as a blowing agent, while simultaneously constructing the PHU network through aminolysis of the cyclic carbonates with cystamine (Scheme 1B). Before investigating foam production, some key features inherent to the presence of cystamine in the formulation had to be considered. The first one was the reactivity of the amine toward 5CC that should be sufficient to promote the crosslinking of the foam. The second one was the plausible dissociation of the disulfide bond under the foaming conditions of the PHU (basic pH and ~100 °C) [57], which might lead to free thiols that are prone to react with 5CC and form irreversible thioether bonds by S-alkylation [33,36]. This effect could prevent the materials expansion due to insufficient crosslinking or inadequate materials viscosity. Thus, the formation of thiols should be avoided to furnish NIPUFs bearing the dynamic disulfide bonds for facilitated covalent adaptable networks (CAN)s abilities. Therefore, the main reactions involved during the production of the foams were first investigated through model studies to identify suitable foaming conditions.

3.1. MODEL REACTIONS

In a preliminary experiment, we monitored the catalyzed reaction between model ethylene carbonate (EC) and cystamine by ^{1}H NMR spectroscopy (Fig. 1A). This study aimed at detecting a possible S-alkylation of cystamine (that could have been generated by in-situ thermal dissociation of cystamine) and at quantifying the yield of EC aminolysis. ^{1}H NMR showed that the signal of EC vanished after about 1 h at 100 °C (Fig. S1). The corresponding urethane product was formed with a yield of 90 % after 180 min (Fig. 1B), confirming the successful aminolysis of EC by cystamine. This reaction was reproduced at 50 and 25 °C (Fig. 1B) with a similar yield (92 and 87 %, respectively). Fortunately, the S-alkylation was not observed, since ^{1}H NMR signals corresponding to hydroxythioether derivatives were absent. The latter was verified by diffusion-ordered spectroscopy (DOSY) NMR of the crude reaction mixture

(Fig. S2). ^{1}H NMR analyses also showed side hydrolysis of EC produced by residual water contaminant (3439 ppm as measured by titration measurements for cystamine), forming ethylene glycol (EG, signal at ~3.3 ppm, Fig. S1). The EG yield remained below 10 % after 180 min at all tested temperatures (red line, Fig. 1B). Based on these results, we could conclude that the aminolysis of cyclic carbonate by cystamine was effective even at room temperature, while preventing the occurrence of S-alkylation. These initial experiments allowed us to anticipate the conditions for producing crosslinked NIPUFs.

Scheme 1. *A) Formulation components, simplified PHU network structure, and B) proposed reaction pathways for NIPUFs via the water-induced self-blowing process. C) Involved network rearrangement mechanisms vs processing temperature range: disulfide exchange, associative transcarbamoylation, and reversible cyclic carbonate formation at elevated temperatures.*

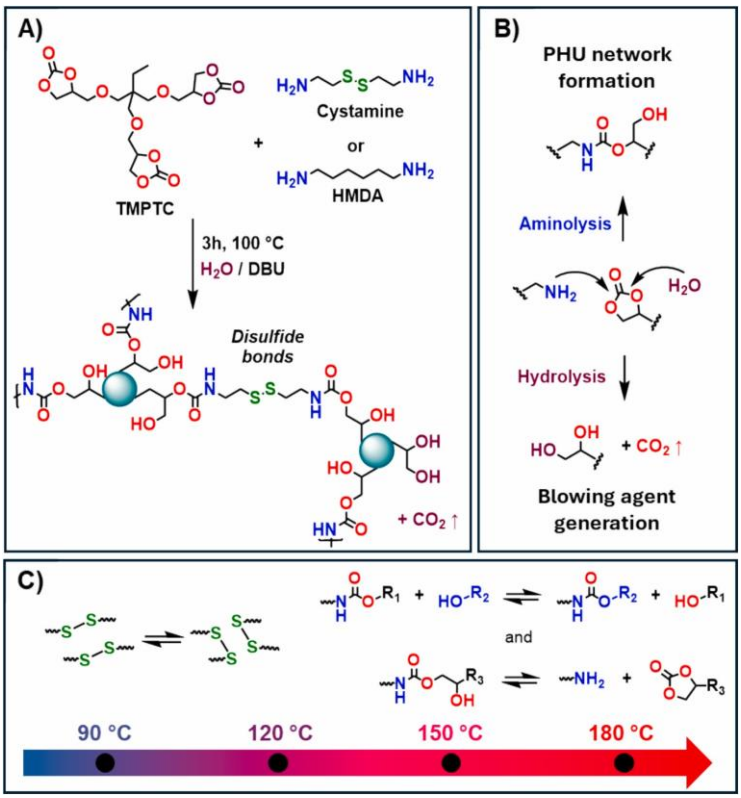

3.2. PREPARATION AND PROPERTIES OF SELF-BLOWN FOAMS

We used a formulation composed of a trifunctional cyclic carbonate (TMPTC), cystamine, water, and DBU catalyst (5 mol % *vs* 5CC groups) (Scheme 1A). Based on previous developments [34], an optimized fixed [amine]/[cyclic carbonate] ([NH_2]/[5CC]) ratio of 0.75 was used to leave 25 mol % of the initial 5CC groups available for hydrolysis, and thus to produce the blowing agent (CO_2) (see Tables S1-S2). Under these conditions, we successfully prepared a foam consisting of 100 % mol of cystamine as hardener with an open-cell porosity, a density of 232 kg m^{-3}, and a high gel content (GC) of 95.6 %, attesting for the crosslinked nature of the foam (Foam A, Fig. 2). FT-IR spectroscopy demonstrated the successful formation of the PHU network with the corresponding appearance of the C = O stretching band of urethane bond (1692 cm^{-1}), N-H bending (1528 cm^{-1}), and O-H stretching (3310 cm^{-1}). The low- intensity C = O stretching band (1789 cm^{-1}) confirmed the consumption of the 5CC groups (Fig. S3).

To evaluate the impact of cystamine on the foaming process and subsequent reprocessing, amine blends including cystamine and the analogue disulfide-free hexamethylenediamine (HMDA) were also

prepared (25, 50, 75 and 100 mol % of HMDA). The morphology and physical properties of the obtained foams are shown in Fig. 2 and Table 1. The increasing ratio of HMDA showed no clear influence on the cell morphology of the foams A-C. When the cystamine ratio was decreased to 25/75 and 0/100, the GC decreased significantly and the cell size increased (Foam E). Although model reactions between EC and both amines exhibited similar aminolysis rates (Fig. 1B and Fig. S4), and the FT-IR spectra of the foams indicated a comparable 5CC conversion into PHU (Fig. S3), the lower GC in the HMDA-rich foam suggests structural heterogeneity, characterized by the presence of weakly cross- linked domains. In line with these observations, increasing the HMDA content in the foams decreased T_g from 29.6 °C (without HMDA) to 15.1 °C (with 100 % HMDA) (Fig. 2B). Nevertheless, all foams exhibit a single glass transition temperature (Fig. 2B), indicating a homogeneous phase for all compositions and falling within the range of previously reported foams containing HMDA (− 2.2 to 18.6 °C) [34]. The observed trend could be further influenced by the more flexible aliphatic chain spacer of HMDA compared to the disulfide spacer in cystamine [50]. Reflecting these results, the 100 %-cystamine Foam A showed a slightly higher compression modulus (*E*) (0.05 ± 0.02 MPa) than foams with an increasing content of HMDA (Fig. 2C), reaching similar values of NIPUFs based on linear amines like EDR 148 and HMDA (0.03 to 0.05 MPa) [34]. Finally, the degradation temperature ($T_{d,5\ \%}$) of cystamine-rich foams (A-C) was measured between 248 and 254 °C, slightly higher than that of 100 %-HMDA foam (Table 1, and Fig. S5). These findings indicate that the cystamine crosslinker can be effectively integrated into NIPUFs without significantly altering the foaming process, while yielding physicochemical properties comparable to those of analogous disulfide-free formulations. Notably, cystamine was incorporated in high contents (up to 100 % cystamine), which, as discussed later, is expected to facilitate the reprocessing of the resulting foams.

Table 1 *Influence of cystamine/HMDA content ratio on the foams properties*

Foam	Cystamine/HMDA	GC [%]	D [kg m^{-3}]	Cell size [mm]	T_g [°C][a]	$T_{d,5\%}$ [°C]	Compression Modulus [MPa][b]
A	100/0	95.6 ± 0.3	232 ± 19	0.88 ± 0.29	29.6	250	0.054 ± 0.016
B	75/25	96.8 ± 0.4	287 ± 14	0.64 ± 0.19	27.1	248	0.045 ± 0.004
C	50/50	89.5 ± 3.2	324 ± 26	0.44 ± 0.11	23.9	254	0.039 ± 0.01
D	25/75	90.4 ± 1.5	379 ± 39	0.33 ± 0.10	20.7	250	0.025 ± 0.005
E	0/100	81.0 ± 4.8	263 ± 29	0.97 ± 0.16	15.1	239	n.d.[c]

[a] *T_g was estimated from the third heating scan (Fig. 2B).*

[b] *Stress strain curves depicted in Fig. 2C.*

[c] *n.d. Sample destroyed during sampling preparation. Compression modulus could not be determined.*

3.3. REPROCESSING OF THE FOAMS

3.3.1. CHARACTERIZATION OF THE CAN BEHAVIOR OF NIPUFS

The NIPU foam-to-film reprocessing was achieved through hot- pressing procedures, which activated the dynamic rearrangement mechanisms within the PHU network as a function of the foam composition and temperature (Scheme 1C). Firstly, the reprocessing conditions were analyzed for Foams A (100 % cystamine) and E (100 % HMDA). Simply heating Foam A in an oven at temperatures ranging from 90 to 140 °C did not result in any evident reprocessing, indicating that applied pressure is necessary to induce rearrangement within the network. Thereafter, Foam A was easily reshaped into a semi- transparent film when maintaining a pressure of 5 Tons at relatively low temperature (90 °C) for 30 min (Fig. S6). Reducing the hot-pressing time to 5 min resulted in an opaque film with a grainy aspect (Fig. S6). In contrast, increasing the temperature to 120 °C under the same conditions yielded a

transparent film with homogeneous aspect (Fig. 3A). On the other hand, the cystamine-free Foam E could not be reprocessed under the same conditions (Fig. S6, 120 °C). In this case, reprocessing the foam into a transparent film required higher temperatures (170 °C) and 5 Tons of pressure, indicating that network rearrangement in this formulation depends on the activation of associative transcarbamoylation within the PHU network. However, these harsher reprocessing conditions may compromise network structure, as partial cyclic carbonate reformation and urea formation can occur [13,58], as evidenced by the increased intensity of their corresponding signals in the FTIR spectrum of the resulting film (Fig. S7).

In contrast to PUFs incorporating low to moderate disulfide bonds contents (disulfide composition 10–50 %, reprocessing at T > 140 °C) [22,23], the high content of cystamine crosslinker in Foams A and B facilitated a rapid reprocessing at 90 or 120 °C. In line with this, foams with lower compositions of cystamine (C-D) could also be reprocessed although longer compression molding times appeared to be required to achieve homogeneous and transparent films. Thereafter, to standardize the process and ensure network rearrangement across all formulations, conditions were set at 120 °C for 30 min with a pressure of 2 Tons. Following this protocol, Foams A to D were successfully reprocessed into crack-free, transparent films (Fig. S8). Since previous reports on the reshaping of PHU foams relying on transcarbamoylation required much higher temperatures (between 140 and 160 °C) for long periods of time and high loading forces [31,36,45], the low reprocessing temperature of cystamine-containing NIPUFs is highly advantageous to facilitate recycling under milder conditions, thereby minimizing side reactions and extending reprocessability.

Cystamine-containing foams were reprocessed several times without any evidence of side reactions altering network structure, as evidenced by FT-IR spectroscopy (see Foam A as an example in Fig. 3A and Fig. S9A). After reprocessing, DSC measurements of the films showed slightly lower T_g values for the foam than the reprocessed films (Fig. S9B). The latter could be attributed to the well-known influence of hydro-plasticization of the foam-structured sample [45,59]. Subsequent reprocessing cycles showed consistent T_g values in the range of 23–24 °C (Fig. S9B, cycle 1–5), confirming that the polymer network maintained its properties under the set conditions of reprocessing for several recycling cycles.

Following the confirmation that the reprocessing conditions did not deteriorate the integrity of the network, stress-relaxation experiments were performed on the obtained films to better understand the underlying phenomena during covalent exchange. Dry-conditioned samples were used for these experiments to discard plasticization effects arising from ambient moisture [50] (see experimental section). The decay of the resulting stress in the material was monitored in the range of temperature from 140 to 90 °C (Fig. S10). The resulting data were fitted to single and two-element Maxwell models for viscoelastic fluids to estimate the relaxation time (τ) of each system, followed by the determination of their energy of activation (E_a) through Arrhenius plots (Fig. 3B). The mathematical fit and experimental data (Fig. S10 and Table S3) showed that the two-element Maxwell model, which considers the contributions of fast and slow exchanging segments within the networks [60], yielded a better fit than the single-element model.

In line with other networks composed of dynamic bonds, the relaxation modulus of the films increased with decreasing temperature (Fig. S10). Comparing the composition of the films, the values of τ and E_a decreased when increasing content of cystamine, which confirmed the correlation between dynamicity of the network and the concentration of disulfide bonds (Fig. 3, Tables S3 and S4).

Interestingly, although permanent cross-links increased for Foam B, E_a showed very similar values to sample A (Fig. 3B, black and red lines), suggesting that the concentration of cystamine could be reduced in the formulation, within the range of 100 to 75 %, without drastically modifying the dynamicity of the network. The latter is especially attractive to modify the properties of the foams, e.g., with different amine crosslinkers, while maintaining reprocessing capabilities. Further decreasing the concentration of cystamine to 50 and 25 % (Foams C and D) displayed a significantly higher τ even when increasing temperature. In this trend, Foam D required a higher temperature range for relaxation (130–160 °C, Fig. 3B, blue line) due to the low content of disulfide bonds. The latter is also reflected on the E_a values of the polymer films. Overall, both fitting models revealed an increasing trend of E_a with the increasing cystamine content in the formulations (Fig. 3C-D and Table S4). The two-element Maxwell model also revealed larger differences between the contribution of fast and slow exchanging segments with the decaying content of cystamine (Fig. 3D). These findings suggest the formation of zones with different exchange rates due to the lower concentration of disulfide bonds within the networks and the activation of the transcarbamoylation and reversible cyclic carbonate mechanism at higher temperatures. In line with previous reports on the reversion of the PHU exchangeable bonds [13,58], exposing a reprocessed film from Foam A to a temperature of 140 °C or higher for 60 min induced side reactions such as the reformation of cyclic carbonates (as evidenced by FT-IR, Fig. S11) and some CO_2 release. This was further supported by the presence of bubbles in samples treated at 175 °C (Fig. S11).

Considering that basic environments are known to trigger disulfide exchange [61], a sample of ground Foam A was washed with methanol to remove residual DBU catalyst from the foam. This sample was dried and hot-pressed under the previously discussed conditions to produce a clear and crack-free film (Fig. S12A). Stress relaxation of the obtained film yielded a slightly higher E_a (79.6 ± 2.9 kJ·mol^{-1}) than the reprocessed "unwashed" foam containing residual DBU (74.4 ± 4.1 kJ·mol^{-1}). This increase on E_a indicated a catalytic effect arising from the presence of DBU during the reprocessing of the unwashed foam. However, removing the catalyst did not prevent reprocessing, as τ values remained in the same range as those of the unwashed sample (Fig. S12B). As demonstrated, disulfide exchange in the networks is accelerated by residual basic catalysts from foaming procedures but can also occur solely through thermal activation under mild conditions, enabling catalyst-free reprocessing.

In this section, we have explored the effects of temperature, pressure, and chemical stimuli (coming from the residual catalyst) on the stress relaxation behavior of the reprocessed films. Several other external factors are known to potentially influence the exchange mechanisms of CANs. Among these, humidity is known to promote hydroplasticization of water-sensitive CANs by increasing molecular mobility and thus accelerating the dynamic bond exchange rate [62,63]. Hydroplasticization of NIPUs is often considered a drawback because it tends to diminish their mechanical properties. As a result, it is primarily exploited only in moisture-healing capabilities [64]. Consistent with these reports, Foam A exhibited moisture uptake (1.8 and 6.1 wt % at 40 and 80 % RH, respectively), leading to a significant reduction in T_g (from 29.6 °C at the dried state to 8 and − 11.5 °C when exposed to 40 and 80 % RH, respectively) and compression modulus (from 0.054 MPa to 0.019 and 0.008 MPa) with limited dimensional change (<3 %, Fig. S13). Intuitively, this susceptibility of NIPU networks to hydroplasticization could also be leveraged to facilitate NIPUFs reprocessability by accelerating covalent bonds exchanges. In the following section, we investigate this hypothesis, using hydroplasticization as a simple, cost-effective tool to reduce relaxation times and facilitate foam reprocessing.

3.3.2. HUMIDITY-FACILITATED REPROCESSING OF PHU FILM

Previous stress relaxation studies were performed on dry- conditioned samples. However, we noticed a plasticization effect induced by ambient moisture on the reprocessed films. As estimated from Fig. 3B (and Table S4), non-conditioned samples composed of 100 % cystamine revealed lower τ and E_a values (gray series) than the analogous conditioned, dried sample (black series). To further investigate this behavior, we subjected films derived from Foam A (100 % cystamine) to controlled conditions of humidity (60 and 80 % RH) and conducted additional stress relaxation experiments at 120 °C to compare with a dried sample. These experiments showed an impressive decrease of the initial G_0 along with a difference of τ in the range of 50 to 350 s according to the humidity conditions (Fig. 4A and C). In line with previous reports on the effect of water in PHU networks [45,50,59], this decreased τ was attributed to the absorption of water by the crosslinked network which diminished H-bonding and increased molecular mobility.

To confirm the practical relevance of water traces during stress relaxation measurements, we performed additional experiments at 90 °C. Again, the decay of G_0 was clear for the moistened sample (from 0.636 MPa at the dried state to 0.202 MPa at the moistened state, Fig. 4B and C, 90 °C). In this case, the decrease of τ was more important (from 7932 s in the dried state to 193 s when moistened), indicating a higher effect of moisture at lower temperatures. These results (90 and 120 °C) show that the dynamicity of the network was accelerated by different combinations of temperature and water content to reach similar τ values. Importantly, FT-IR monitoring of the drying-humidity cycles showed no significant effects on the network's chemical structure (Fig. S14). In good accordance with these observations, DSC exhibited the significant decrease of the film's T_g after humidity at 80 % (− 12,4 °C), which was effectively recovered after drying the sample (26.7 *vs* 28.5 °C, Fig. S15). Overall, hydroplasticization accelerated the rearrangement of the network, a crucial asset for reprocessing foam materials.

Given the influence of moisture during stress relaxation of the films, we investigated the reprocessing of a moistened foam via hot-pressing. Thus, a ground sample of Foam A with 80 % RH (9.7 % H_2O uptake, as determined by TGA) was easily reprocessed at 90 °C for 30 min (2 Tons), yielding a more homogeneous, transparent film than its dried counterpart (Fig. 5). Increasing hot-pressing time improved the homogeneity and transparency for moistened samples (1 and 2 h, Fig. 5). SEM micrographs revealed a uniform and compact morphology without detectable cracks, voids or phase separation (Fig. 5). The absence of significant defects suggests comparable film-forming capabilities between dried and moistened samples. To further test the role of humidity, dry-conditioned and moistened samples of disulfide-free Foam E (100 % HMDA) were also analyzed aiming to decrease their reprocessing temperature. In sharp contrast to the cystamine-rich sample, the dried HMDA-rich sample delivered opaque films at 140 °C after 4 h (5 Tons) and could only be reprocessed at a temperature of 170 °C (Fig. S16). Meanwhile, the moistened sample (11.7 % H_2O uptake, 80 % RH) yielded relatively transparent films at 140 °C from 2 and 4 h of hot pressing (5 Tons, Fig. S16). These experiments confirmed that hydroplasticization facilitated the polymer network reorganization and thus the foam-to-film reprocessing of NIPUFs through different dynamic exchange mechanisms. This effect provides an accessible and effective way to reprocess NIPU materials without recurring to the elevated temperatures or catalysts required for conventional PUs.

3.4. FOAM-TO-ADHESIVE RECYCLING

Depending on their composition, PHU prepared by curing reactive formulations on various substrates have demonstrated to present good to excellent adhesion, making them suitable for a wide range of adhesive applications [55,65–67]. In this work, we evaluated the potential of the substrates to be glued (standard stainless steel, glass, and nylon fabric). reprocessed films to be used as debondable adhesives. Adhesion per- Then, standard lap-shear tests were performed to evaluate the adheformance was assessed by simply hot-pressing the films between the sive's lap-shear strength (LSS) and compare it with commercially available formulations.

3.4.1. ADHESIVE PERFORMANCE FOR STAINLESS STEEL AND GLASS SUBSTRATES

As a first approach, the LSS of dried films obtained from reprocessed foams was evaluated by bonding standard stainless-steel substrates at 120 °C for 10–30 min (0.5 Ton) to monitor the effect of adhesive composition and welding time (Fig. 6A-B and Fig. S17). Results showed that the disulfide bond content in the adhesive film was critical for adhesion performance: increasing the cystamine content led to improved LSS, from 1.2 ± 0.7 MPa (50 % cystamine) and 1.6 ± 0.7 MPa (75 % cystamine) to 2.6 ± 0.2 MPa (100 % cystamine) after a 30-minute welding time. In line with previous reports on PU thermosets with varying disulfide contents [20,21], this enhancement in LSS values is likely due to faster network rearrangement, as supported by stress relaxation data. In contrast, formulations with 75 % and 50 % cystamine appeared to require longer welding times to achieve full network reorganization. When processed under shorter welding times (30 min), these formulations yielded heterogeneous films and, consequently, premature adhesive failure. As a result, lower cystamine contents also led to more variable adhesion data. Further decreasing the cystamine content to 25 % and 0 % (Foams D and E, respectively) resulted in no adhesion under the tested welding conditions. While formulations A-C delivered LSS values considered as high-performance adhesives [68], following experiments were performed using the film derived from foam A (100 % cystamine) as it showed the highest LSS along with cohesive-type failures (Fig. S17). Thus, we attempted to optimize the welding time for this NIPU adhesive. In line with our previous discussion, reducing welding time to 10 min resulted in a LSS of 1.8 ± 1.0 MPa with a large standard deviation (green series, Fig. 6B). In comparison, extending the welding time to 4 h yielded LSS values with lower data variability (2.7 ± 0.2 MPa, red series, Fig. 6B) similar to the 30-minutes conditions (blue series, Fig. 6B). In good accordance with previous reports on other types of CAN adhesives [52,69], this preliminary analysis emphasized the importance of activating the network's dynamic chemistry to enable rearrangements and consequently improve adhesive-surface contact under optimal conditions.

The strength performance of the reprocessed films was also benchmarked against commercially available adhesives (Fig. 6C): Ethyl cyanoacrylate (ECA, SuperGlue), hot melt EVA (HM), and PU prepolymer adhesives (PU). To ensure an equivalent comparison between the different formulations, benchmark adhesives were tested under the application conditions recommended by their manufacturers (see experimental section). Therefore, under the optimized conditions (100 % cystamine, 30 min welding, 0.5 Tons), the NIPU adhesive exhibited a higher LSS on stainless-steel substrates (2.7 ± 0.2 MPa) compared to HM (1.4 ± 0.4 MPa) and PU-based adhesives (1.1 ± 0.1 MPa). Due to the irreversible crosslinking on the substrate, the ECA-based adhesive yielded the highest LSS among all formulations (6.2 ± 0.7 MPa), however limiting its recyclability.

In this regard, the network's rearrangement capability of the NIPUF- derived adhesive brings practical relevance since it could be exploited as a formulation with reversible adhesion. Thus, the NIPU adhesive was recovered after the first lap-shear test and subsequently welded (120 °C, 0.5 Tons, 30 min) onto fresh steel plates for a new lap-shear measurement (see experimental section for details). After each test, the adhesive was recycled in the same manner for additional adhesion cycles (Fig. 6C-D). Interestingly, the recycled adhesive showed an enhanced performance with respect to the first test (from 2.6 ± 0.2 MPa to 5.7 ± 1.0 MPa; Fig. 6C). The adhesive cycle was repeated once more rendering a LSS of 4.7 ± 1.2 MPa with a cohesive failure (Fig. 6D), indicating an enhanced adhesive-surface interaction after reusing the adhesive. As attested by FT-IR (Fig. S18), the crosslinked network showed integrity through multiple adhesion-recycling cycles. Thus, consistent with previous studies on disulfide adaptable networks [50,70–73], the enhanced adhesive performance could be attributed to the dynamicity of disulfide bonds, which reform crosslinks after each reprocessing cycle. Regarding adhesion applications, this process could reduce network defects through stress redistribution, allowing material restoration while slightly increasing LSS after recycling.

In a similar fashion, HM adhesives based on thermoplastic polymers such as EVA can display reversible adhesion. Although these adhesives have a wide range of applications in many sectors, such as food packaging, carton-sealing, electronics and textile manufacturing, to cite a few relevant applications [66,74], their low melting temperature limits their performance, making them only suitable primarily for hold-in-place operations with minimal load demands [74]. To evaluate if our adhesive could surpass this limitation, creep tests were conducted under constant stress at a temperature above the polymers' T_g. For CANs, creep has also been considered a drawback due to their intrinsic dynamic covalent nature. In practical applications, bond exchange should be rapid and highly active during high temperature processing, but remain slow and inactive under standard conditions to effectively minimize creep [75].

As shown in Fig. 7A, the HM benchmark demonstrated an instantaneous strain after applying stress (>2.5 % after 10 s) at 50 °C. Later, after 8 h of constant stress, the creep strain ($\Delta\varepsilon$) increased up to 0.24, highlighting the significant creep behavior of this adhesive. In contrast, the NIPU adhesive showed a significantly lower instantaneous strain (<1 %), effectively restraining creep ($\Delta\varepsilon$ = 0.016), thus indicating that the network kept dimensional stability at 50 °C for 8 h. Finally, when the stress was removed, the HM adhesive partially recovered strain (0.024 after 2h of removing stress). In contrast, the minimal residual strain for the NIPUF-derived film demonstrated almost full recovery. The significant difference in creep strain behavior is consistent with the crosslink density of the PHU network with practically no dissociation of disulfide bonds at this temperature [76], which could however be activated on demand at higher temperatures.

Building on this concept, unlike permanently crosslinked adhesives such as ECA or PU, the thermal reprocessability of NIPUF-derived adhesives could enable practical heat-triggered debonding. A proof-of- concept test consisted of heating a joint glued with NIPU adhesive using a heat gun while applying a force to assess the joint separation. To analyze this property, uniaxial creep tests on stainless-steel joints (25–60 °C, Fig. 7B) showed that stabilized creep strains were achieved at 25 °C under loading forces of 0.1 to 0.2 kN (creep strain = 0.35 and 0.81, respectively), indicating a theoretical weight support up to ~20 kg/cm^2. Stabilized creep strain could be extended to 40 °C by decreasing the loading force from 0.1 kN (with a failure after 1000 s) to 0.05 kN (theoretical weight support ~5.1 kg/cm^2); no failure was observed after 2000 s. Beyond that, increasing the temperature to 60 °C resulted in a creep

strain exceeding 1.3 % after 2,000 s. As shown, temperature and loading force directly influenced the adhesion performance, offering practical means for thermally debonding joint samples.

The NIPUF-derived adhesive was also evaluated for gluing glass substrates (green series, Fig. 6C), showing an adhesive-type failure (Fig. S19). Importantly, the adhesive could be reused multiple times with similar performance (1st cycle: 0.8 ± 0.1 MPa, 2nd cycle: 0.9 ± 0.2 MPa, and 3rd cycle: 0.9 ± 0.1 MPa). LSS remained lower in comparison to stainless-steel surfaces in the same number of adhesion cycles, nevertheless still remained in the range of the benchmark adhesives: HM (1.1 ± 0.2 MPa), PU (1.2 ± 0.4 MPa), and ECA (1.3 ± 0.3 MPa). This relatively strong adhesion of the NIPU adhesive to glass and stainless- steel substrates was further evaluated using the widely applied glass- stainless steel connection [77]. Commercial adhesives for such connections typically comprise two-component formulations that require chemical curing to achieve high stiffness. However, these systems often suffer from complex preparation, high strength variability, limited flexibility and ductility, and restricted recyclability [78]. In contrast, the reprocessed NIPU film enabled a straightforward steel-glass bonding process, requiring only hot pressing the adhesive between the substrates (4 h, 120 °C, 0.5 Tons). The LSS of the NIPU film (4.6 ± 1.0 MPa) significantly outperformed PU (0.7 ± 0.1 MPa) and HM (1.1 ± 0.3 MPa) benchmarks, while closely approaching the ECA formulation (5.6 ± 0.2 MPa) (Fig. 8A). Although inconsistent failure types were observed (Fig. 8B), these results showcase the adhesion potential of the reprocessed NIPU adhesives.

It has to be noted that adhesion performance is highly sensitive to experimental factors such as substrate pre-treatment, application conditions, and testing protocols [68,79,80]. For instance, sanding the substrate more than doubled the LSS of the NIPU adhesive on stainless steel, reaching 6.5 ± 0.5 MPa (Fig. S20). While commonly used [80,81], sanding protocols vary widely, limiting reproducibility and cross-study comparisons. As such, comparing LSS values across different studies is unreliable unless test conditions are identical, which is rarely the case. Instead, benchmarking new adhesives against commercial ones under the same conditions offers a more meaningful assessment of performance. In summary, our benchmarking study shows that our solvent- free, one-component NIPU adhesive matches commercial performance while offering on-demand debonding and recyclability—advantages over conventional thermosets.

3.4.2. ADHESIVE PERFORMANCE FOR NYLON FABRICS

Conventional PU are widely used in the textile sector, particularly as coatings and adhesives. However, despite their good performance, the reliance on solvent-based formulations and the chemicals used during their production limit their applications [67,82]. In contrast, the recyclable, one-component NIPU adhesive offers a solvent-free alternative with strong adhesion, making it a suitable candidate for textile bonding applications. To assess its potential, a reprocessed film derived from Foam A (100 % cystamine) was welded onto nylon fabric at 120 °C for 30 min (Fig. 9A). Scanning electron microscopy (SEM) images revealed uniform impregnation of the adhesive into the fabric (Fig. 9B-C and Fig. S21). The obtained composite was then cut into strips, welded at an overlapped area of 100 mm^2, and evaluated by lap-shear tests (Fig. 9A).

The adhesive performance of the NIPU film was assessed by benchmarking against the previous commercial adhesives (ECA, HM and PU), including a natural rubber-based adhesive (NR) specifically engineered for textiles (Fig. 9D). After evaluating the impact of welding time and temperature (Figs. S22A and S23), initial conditions of 120 °C and 140 °C for 30 min were selected. Thus, the NIPU adhesive achieved LSS values of 1.4 ± 0.2 MPa at 120 °C and 1.2 ± 0.2 MPa at 140 °C (Fig. 9D), indicating excellent

adhesion performance under these conditions. Additionally, aiming to reduce the welding time (Fig. S22B), the temperature was increased to 160 °C, yielding similar LSS values (1.0 ± 0.2 MPa) after just one minute of welding. As expected, elevated temperatures allowed for a faster exchange rate that accelerated the rearrangement of the network [71]. Furthermore, as shown by the partial destruction of the fibers after lap-shear tests (Fig. 9E), this faster rearrangement promoted the penetration of the adhesive through the fibers (Fig. 9B-C and Fig. S21) underscoring a strong adhesive bonding with cohesive failures. This quick welding process surpassed the LSS of the specialized NR adhesive (0.8 ± 0.1 MPa), while reaching comparable values to HM and EC benchmarks (Fig. 9D). The PU benchmark outperformed all formulations, but the assembly required a curing time of 4h. In comparison, welding times as short as 1 min were achieved for the NIPU adhesive at 120–160 °C, with an expected increase of adhesion performance with temperature (Fig. S22B), and partial destruction of the substrates after the lap-shear tests (Fig. 9E). Notably, LSS stress–strain curves exhibited a characteristic higher strain at break for the NIPU adhesive (30, 39, and 54 %, for 120, 140 and 160 °C, respectively) than the best-performing benchmarks (*e.g.*, 34 and 48 % for ECA and PU, respectively, Fig. S24). This behavior reflects the known strong adhesion performance of permanently crosslinked adhesives, but low work of debonding due to their inherent brittleness [83]. In contrast, the incorporation of temperature-activated disulfide bonds in the formulation provides strong adhesion strength at short welding times while delivering ductility. These properties are critical for practical purposes in the textile industry, where flexibility, toughness, and straightforward application are essential [83].

4. Conclusions

This study introduces an effective approach to prepare self-blown thermoset NIPUFs with facilitated reprocessability into recyclable and on-demand detachable adhesives for multiple substrates. Incorporating disulfide covalent dynamic bonds, using cystamine as crosslinker, into water-induced self-blown NIPUFs enabled their foam-to-film reprocessing under mild treatment (as low as 90 °C under a low loading force), even under catalyst-free conditions. Furthermore, we demonstrated that hydroplasticization served as an effective tool to facilitate and accelerate the reprocessing of the NIPU networks. Starting from NIPUFs or films, hydroplasticization significantly influenced T_g, G_0, and τ, enabling the reprocessing of NIPU networks with cystamine or HMDA crosslinkers at lower temperatures than their dried counterparts. Importantly, the synergy between disulfide bonds and hydroplasticization enabled rapid processing at just 90 °C within 30 min, with tunable network relaxation via water content. This marks a major advance over conventional methods requiring T >140 °C, high pressure, and extended processing times. The reprocessed cystamine-containing films were utilized as film adhesives for stainless steel and glass substrates offering a convenient, one-component adhesive applied via hot pressing. By adjusting welding time and temperature, the recyclable cystamine-rich NIPU adhesive showed competitive performance against commercial formulations such as hot-melt and thermoset adhesives (including the standard ethyl cyanoacrylate Super Glue), while providing advantageous properties, including ease of application, reversible adhesion, creep resistance, heat-triggered debondability, ductility, and recyclability. These features were particularly useful for complex connections such as stainless steel- glass or nylon fabrics, maintaining adhesion performance. The introduced foam-to-adhesive procedure highlights the versatility of disulfide-modified NIPUFs and the importance of moisture on recycling, expanding their potential applications in a wide range of PU-based applications without compromising recyclability. Beyond enabling the

production of easily recyclable NIPU foams, this study demonstrates how the synergistic interaction between hydroplasticization and dynamic disulfide bonds enables facile, efficient, and cost-effective recycling and repurposing of NIPU networks.

Credit authorship contribution statement

Víctor D. Lechuga-Islas: Writing – original draft, Visualization, Validation, Methodology, Investigation, Formal analysis, Data curation, Conceptualization. **Emeline Gillissen:** Writing – original draft, Visualization, Investigation, Methodology, Formal analysis. **Maxime Bourguignon:** Writing – original draft, Supervision, Methodology, Conceptualization. **Bruno Grignard:** Writing – review & editing, Supervision, Methodology, Investigation, Conceptualization. **Christophe Detrembleur:** Writing – review & editing, Validation, Supervision, Project administration, Methodology, Investigation, Funding acquisition, Conceptualization.

Declaration of competing interest

The authors declare the following financial interests/personal relationships which may be considered as potential competing interests: Christophe Detrembleur reports financial support was provided by Walloon Region. Christophe Detrembleur reports financial support was provided by Fund for Scientific Research. Christophe Detrembleur reports a relationship with Fund for Scientific Research that includes: employment, funding grants, and travel reimbursement. Christophe Detrembleur, Maxime Bourguignon and Bruno Grignard have patent #WO2023/104362: Self-blowing isocyanate-free polyurethane foams pending to University of Liege. If there are other authors, they declare that they have no known competing financial interests or personal relationships that could have appeared to influence the work reported in this paper.

Acknowledgements

The authors thank the Region Wallonne for funding the Win2Wal project “ECOFOAM” (convention 2010130) and the FRFS-WEL-T Advanced Grant project “Chemistry” (convention WEL-T-CR-2023 A). Christophe Detrembleur is FNRS Research Director and thanks the “Fonds de la Recherche Scientifique (F.R.S.-FNRS, Belgium) for funding. A preprint of this article appeared on ChemRxiv at DOI: 10.26434/chemrxiv-2025-hl2k7. Patent pending (WO2023/104362: Self-blowing isocyanate-free polyurethane foams).

Appendix A. Supplementary data

Supplementary data to this article can be found online at https://doi. org/10.1016/j.cej.2025.163998.

Data availability

Supplementary data are available in Supporting Information.

Figures

Fig. 1. *Aminolysis, hydrolysis and S-alkylation pathways of EC in the presence of cystamine: A) Scheme of reactions and B) Estimated yield of products at different temperatures in the presence of DBU (0.05 eq vs 5CC groups).*

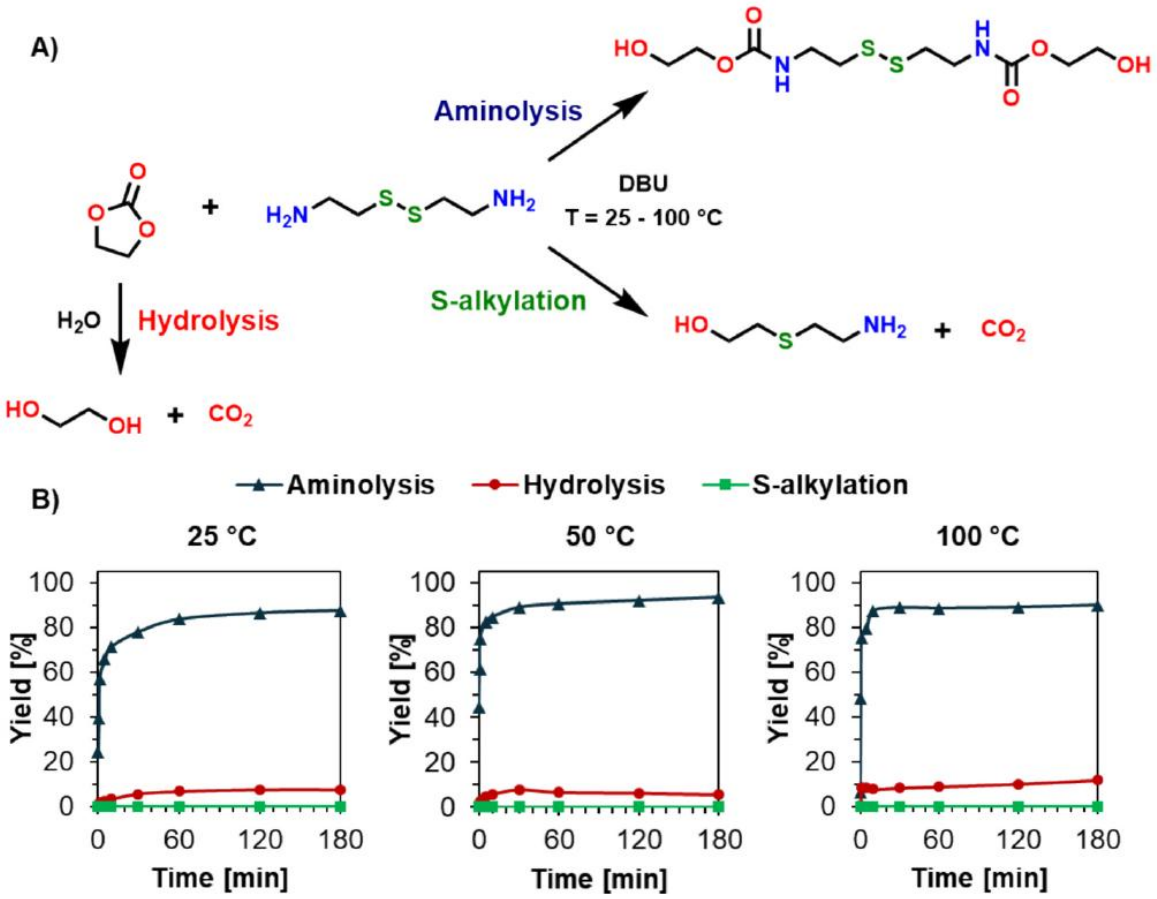

Fig 2. *A) Photography and SEM images of the foams with variable cystamine/HMDA ratio. B) DSC thermograms of the dried foams. Tg values were obtained from the third heating scan. C) Compression stress–strain curves of dried Foams A-D.*

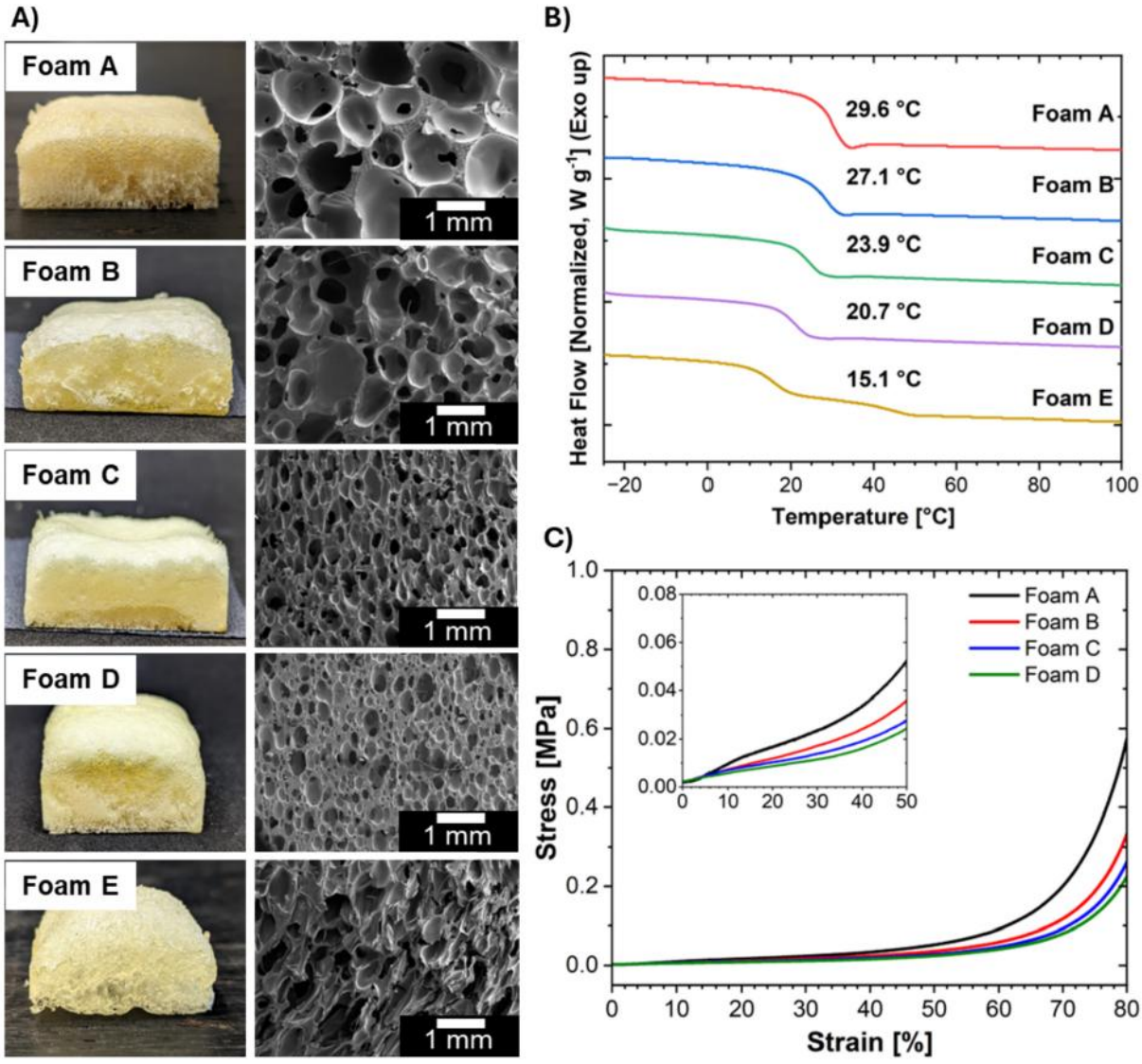

Fig. 3. *A) Reprocessing of the ground Foam A by hot pressing (initial ground foam (left), crack-free film (middle) and recycled film after one to three cycles (right)). B) Arrhenius temperature dependence of average stress relaxation times (estimated by the single Maxwell model) according to cystamine composition for dried samples (non-conditioned sample (gray squares) was not dried prior analysis). Overview of the estimated Ea values as a function of cystamine composition using a single (C) and double Maxwell model (D) (see stress relaxation curves and fitted curves are shown in Fig. S10).*

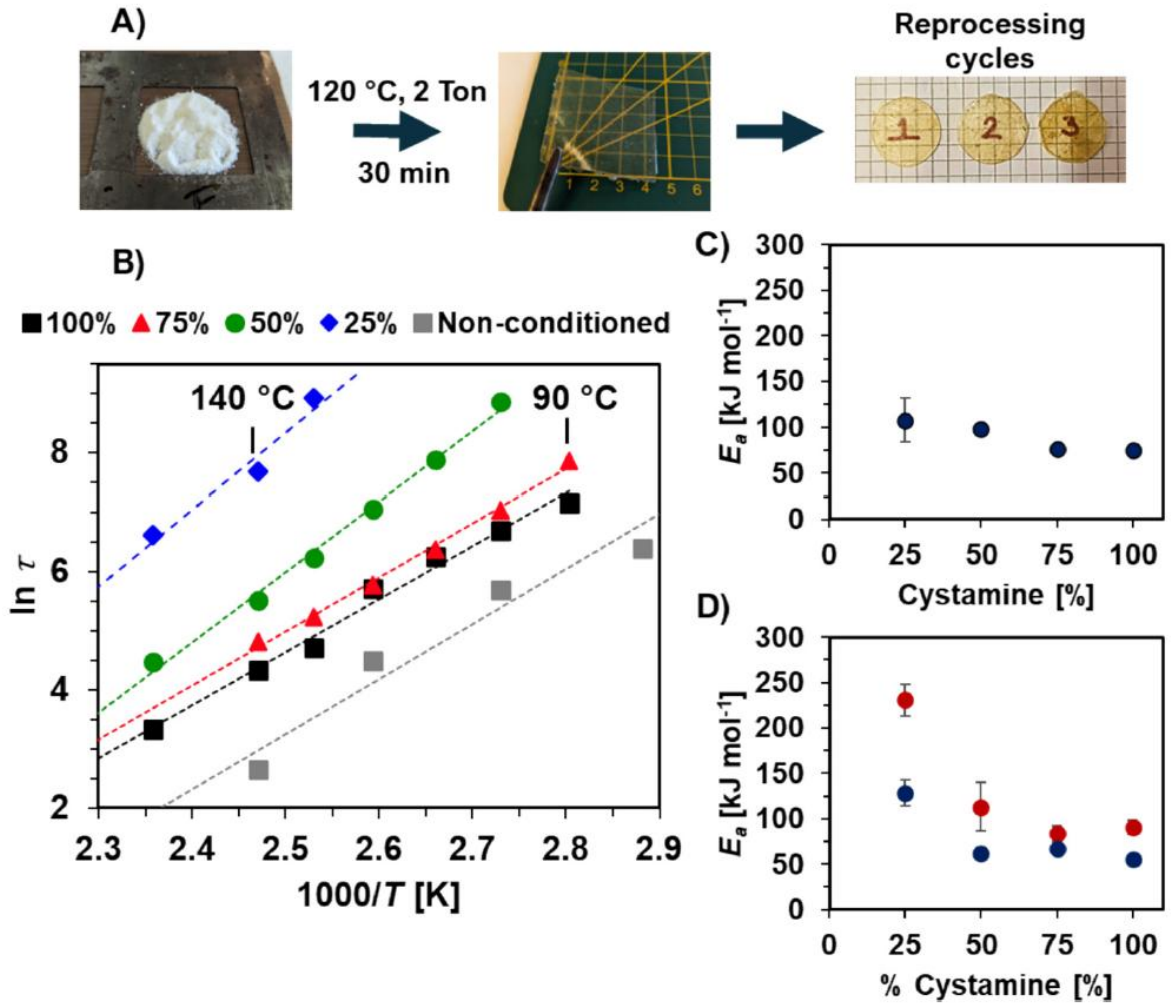

Fig. 4. *Humidity effect on film samples derived from Foam A (100 % cystamine): A) stress relaxation curves at 120 ◦C of dried and moistened films (RH of 60 and 80 %), B) stress relaxation at 90 ◦C of dried and moistened films (RH of 80 %), and C) overview of the G0, τ, and R2 values estimated by a double-Maxwell Model.*

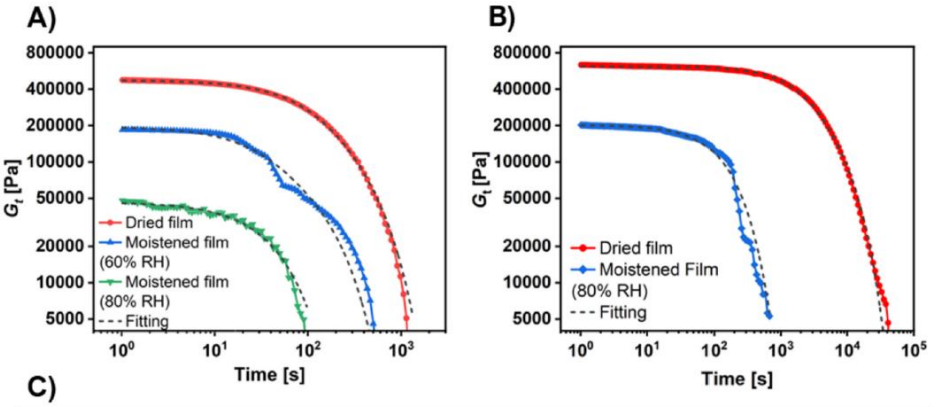

C)

Film sample	H_2O Uptake [%]	Stress relaxation [°C]	G_0 [MPa]	τ_1 [s]	τ_2 [s]	R^2
Dried	-	120	0.474	350	101	0.999
Moistened (60% RH)	4.7	120	0.185	142	32	0.995
Moistened (80% RH)	5.9	120	0.048	49	49	0.986
Dried		90	0.636	7,932	2,222	0.998
Moistened (80% RH)	6.8	90	0.202	193	193	0.987

Fig. 5. *Resulting films from processing foam A (100 % cystamine) under varying drying and RH conditions. SEM micrographs show film morphology after 2 h of hot pressing.*

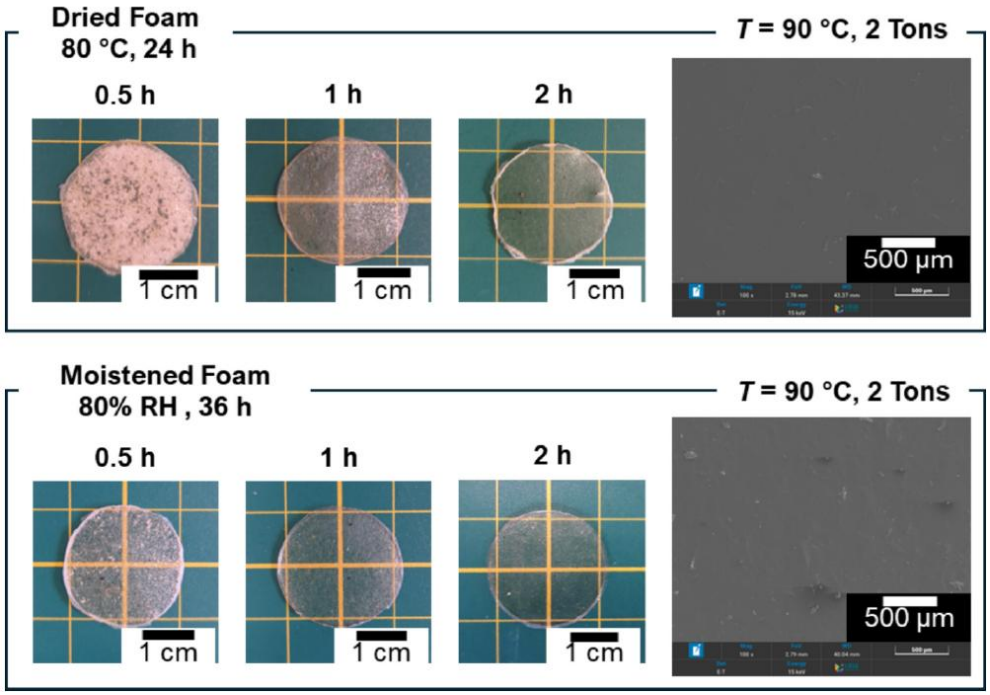

Fig.6. *A) and B) Influence of the cystamine content (50–100 %) and welding time (T = 120 ◦C, 0.5 Tons) on the adhesive performance of reprocessed foams on stainless steel substrates. C) LSS of NIPU adhesive (100 % cystamine) for 1 to 3 adhesion-recycling cycles and benchmarking against various commercially available adhesives on glass and stainless-steel substrates. D) Representative failure type of NIPU adhesive (100 % cystamine) after 1–3 adhesive cycles on stainless steel substrates (welding conditions: 120 ◦C, 0.5 Tons, 30 min).*

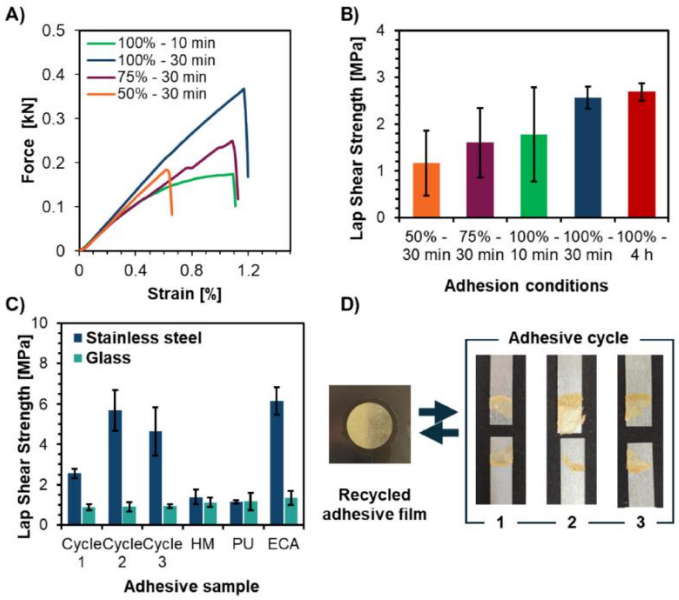

Fig. 7. A) Creep curves for the 100 %-cystamine NIPU film (black line) and the HM adhesive (red line) at 50 °C experiencing a 3.0 kPa shear stress. B) Uniaxial creep test of stainless-steel substrates joined by a 100 %-cystamine NIPU film (derived from Foam A) at different temperatures and loading forces.

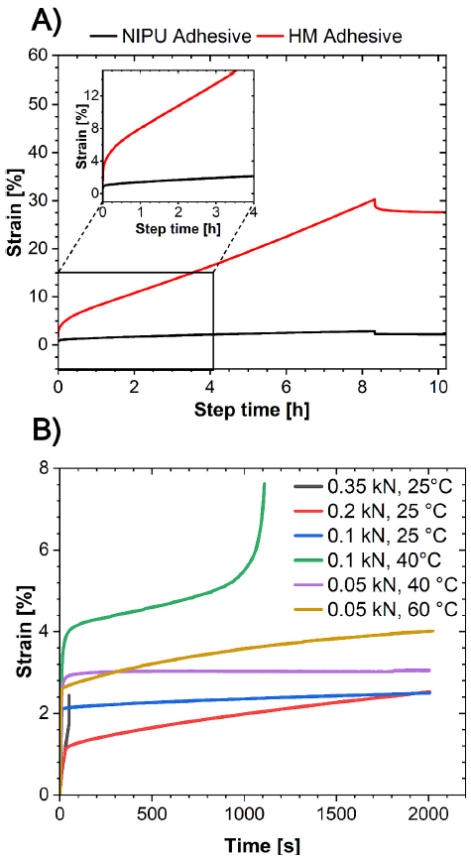

Fig. 8. *A) LSS measurements of the NIPU adhesive (100 % cystamine (4 h, 120 °C, 0.5 Tons)) and benchmarks on stainless steel-glass joints. B) Failure types observed for bonded stainless steel-glass joints bonded with NIPU film.*

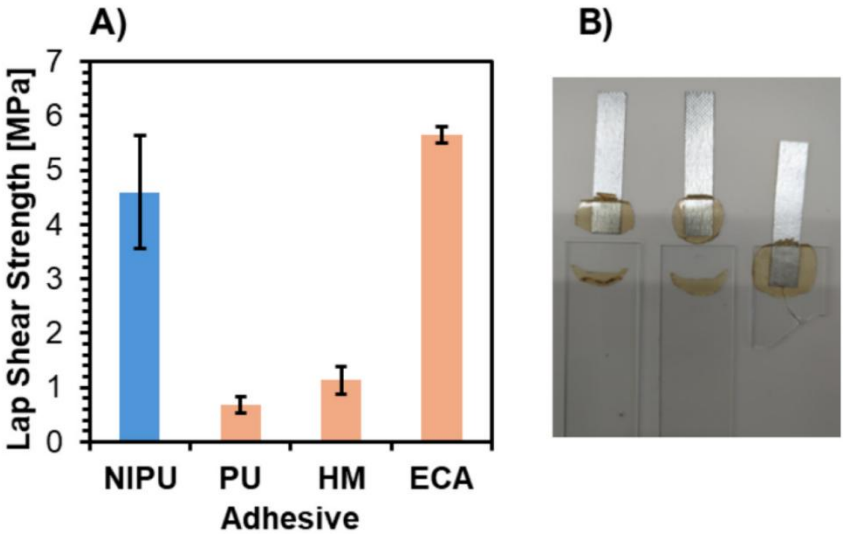

Fig. 9. *A) Representative fabrication of the nylon fibers/NIPU composite by hot pressing. Representative SEM transversal view of a nylon fabric before (B) and after composite fabrication (welding 120 ◦C, 60 min, 0.5 Tons) (C). Complementary micrographs in Fig. S21. D) LSS of joint nylon fabrics welded at various times and temperatures and benchmarking to commercial adhesives. E) Representative failure type of NIPU adhesive applied at 120–160 ◦C welding temperatures for one minute.*

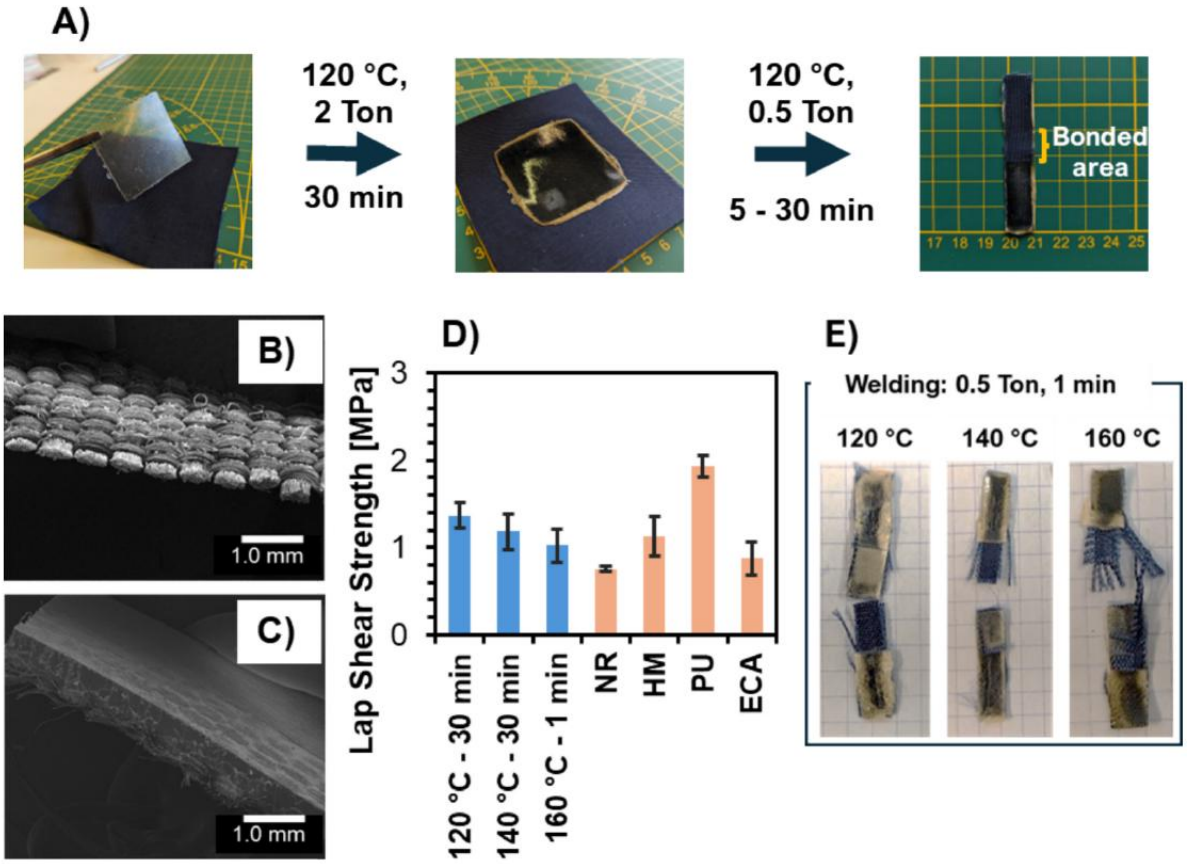

References

[1] A.Delavarde, G. Savin, P. Derkenne, M. Boursier, R. Morales-Cerrada, B. Nottelet, J. Pinaud, S. Caillol, Sustainable polyurethanes: toward new cutting-edge opportunities, Prog. Polym. Sci. 151 (2024) 101805, https://doi.org/10.1016/j.progpolymsci.2024.101805.

[2] C. Liang, U.R. Gracida-Alvarez, E.T. Gallant, P.A. Gillis, Y.A. Marques, G. P. Abramo, T.R. Hawkins, J.B. Dunn, Material flows of polyurethane in the United States, Environ. Sci. Technol. 55 (2021) 14215–14224, https://doi.org/10.1021/ acs.est.1c03654.

[3] J. Niesiobędzka, J. Datta, Challenges and recent advances in bio-based isocyanate production, Green Chem. 25 (2023) 2482–2504, https://doi.org/10.1039/ D2GC04644J.

[4] J. Peyrton, L. Av´erous, Structure-properties relationships of cellular materials from biobased polyurethane foams, Mater. Sci. Eng. R. Rep. 145 (2021) 100608, https://doi.org/10.1016/j.mser.2021.100608.

[5] M. Ates, S. Karadag, A.A. Eker, B. Eker, Polyurethane foam materials and their industrial applications, Polym. Int. 71 (2022) 1157–1163, https://doi.org/ 10.1002/PI.6441.

[6] F. Monie, T. Vidil, B. Grignard, H. Cramail, C. Detrembleur, Self-foaming polymers: Opportunities for the next generation of personal protective equipment, Mater. Sci. Eng. R. Rep. 145 (2021) 100628, https://doi.org/10.1016/j.mser.2021.100628.

[7] B. Liu, Z. Westman, K. Richardson, D. Lim, A.L. Stottlemyer, T. Farmer, P. Gillis, V. Vlcek, P. Christopher, M.M. Abu-Omar, Opportunities in closed-loop molecular recycling of end-of-life polyurethane, ACS Sustain. Chem. Eng. 11 (2023) 6114–6128, https://doi.org/10.1021/acssuschemeng.2c07422.

[8] J.O. Akindoyo, M.D.H. Beg, S. Ghazali, M.R. Islam, N. Jeyaratnam, A.R. Yuvaraj, Polyurethane types, synthesis and applications – a review, RSC Adv. 6 (2016) 114453–114482, https://doi.org/10.1039/C6RA14525F.

[9] D.T. Sheppard, K. Jin, L.S. Hamachi, W. Dean, D.J. Fortman, C.J. Ellison, W. R. Dichtel, Reprocessing postconsumer polyurethane foam using carbamate exchange catalysis and twin-screw extrusion, ACS Cent. Sci. 6 (2020) 921–927, https://doi.org/10.1021/acscentsci.0c00083.

[10] M. Sun, D.T. Sheppard, J.P. Brutman, A. Alsbaiee, W.R. Dichtel, Green catalysts for reprocessing thermoset polyurethanes, Macromolecules 56 (2023) 6978–6987, https://doi.org/10.1021/acs.macromol.3c01116.

[11] B. Quienne, F. Cuminet, J. Pinaud, M. Semsarilar, D. Cot, V. Ladmiral, S. Caillol, Upcycling biobased polyurethane foams into thermosets: toward the closing of the loop, ACS Sustain. Chem. Eng. 10 (2022) 7041–7049, https://doi.org/10.1021/ acssuschemeng.2c00950.

[12] S. Kim, J.L. Swartz, O. Sala, M. Sun, A.K. Oanta, J.P. Brutman, A. Alsbaiee, W. R. Dichtel, Thermal activation of Zirconium(IV) acetylacetonate catalysts to enhance polyurethane synthesis and reprocessing, Macromolecules 57 (2024) 6759–6768, https://doi.org/10.1021/acs.macromol.4c00625.

[13] C. Bakkali-Hassani, D. Berne, V. Ladmiral, S. Caillol, Transcarbamoylation in polyurethanes: underestimated exchange reactions? Macromolecules 55 (2022) 7974–7991, https://doi.org/10.1021/acs.macromol.2c01184.

[14] A. Bandegi, M. Montemayor, I. Manas-Zloczower, Vitrimerization of rigid thermoset polyurethane foams: A mechanochemical method to recycle and reprocess thermosets, Polym. Adv. Technol. 33 (2022) 3750–3758, **https://doi.org/10.1002/pat.5827**.

[15] S. Kim, K. Li, A. Alsbaiee, J.P. Brutman, W.R. Dichtel, Circular Reprocessing of thermoset polyurethane foams, Adv. Mater. 35 (2023) 2305387, https://doi.org/10.1002/adma.202305387.

[16] K. Zhong, Q. Guan, W. Sun, M. Qin, Z. Liu, L. Zhang, J. Xu, F. Zhang, Z. You, Hot- melt adhesive based on dynamic oxime-carbamate bonds, Ind. Eng. Chem. Res. 60 (2021) 6925–6931, https://doi.org/10.1021/acs.iecr.1c00768.

[17] S. Wang, Z. Liu, L. Zhang, Y. Guo, J. Song, J. Lou, Q. Guan, C. He, Z. You, Strong, detachable, and self-healing dynamic crosslinked hot melt polyurethane adhesive, Mater. Chem. Front. 3 (2019) 1833–1839, https://doi.org/10.1039/C9QM00233B.

[18] H. Kassem, E.H. Samat, L. Imbernon, F.E. Du Prez, Foam-to-foam recycling potential of PU-foams by integration of amino esters, Adv. Funct. Mater. 34 (2024) 2409263, https://doi.org/10.1002/adfm.202409263.

[19] K. Unal, D. Maes, L. Stricker, K. Lorenz, F.E. Du Prez, L. Imbernon, J.M. Winne, Foam-to-elastomer recycling of polyurethane materials through incorporation of dynamic covalent TAD-indole linkages, ACS Appl. Polym. Mater. 6 (2024) 2604–2615, https://doi.org/10.1021/acsapm.3c02791.

[20] X.Z. Wang, M.S. Lu, J.B. Zeng, Y. Weng, Y.D. Li, Malleable and thermally recyclable polyurethane foam, Green Chem. 23 (2021) 307–313, https://doi.org/10.1039/ d0gc03471a.

[21] W. Liu, Y.C. Chang, C. Hao, H. Liu, J. Zhang, D. Mielewski, A. Kiziltas, Improving thermal reprocessability of commercial flexible polyurethane foam by vitrimer modification of the hard segments, ACS Appl. Polym. Mater. 4 (2022) 5056–5067, https://doi.org/10.1021/acsapm.2c00595.

[22] C. Zhang, H. Liang, D. Liang, Z. Lin, Q. Chen, P. Feng, Q. Wang, Renewable castor- oil-based waterborne polyurethane networks: simultaneously showing high strength, self-healing, processability and tunable multishape memory, Angew. Chem. Int. Ed. 60 (2021) 4289–4299, https://doi.org/10.1002/ANIE.202014299.

[23] H. Zhou, C. Liu, J. Huang, Y. Li, G. Zhu, C. Lu, J. Yao, H. Xu, P. Zhao, High- performance, high biobased content, self-repairable, and recyclable biobased photopolymers for UV-curing 3D printing, Ind. Crop. Prod. 224 (2025) 120299, https://doi.org/10.1016/J.INDCROP.2024.120299.

[24] Y. Zeng, J. Li, C. Hu, B. Yang, Z. Ning, Sustainable polyurethane networks with high self-healing and mechanical properties based on dual dynamic covalent bonds, Macromol. Chem. Phys. 224 (2023) 2200322, https://doi.org/10.1002/ MACP.202200322.

[25] H. Blattmann, M. Lauth, R. Mülhaupt, Flexible and bio-based nonisocyanate polyurethane (NIPU) foams, Macromol. Mater. Eng. 301 (2016) 944–952, https:// doi.org/10.1002/mame.201600141.

[26] B. Grignard, J.-M. Thomassin, S. Gennen, L. Poussard, L. Bonnaud, J.-M. Raquez, P. Dubois, M.-P. Tran, C.B. Park, C. Jerome, C. Detrembleur, CO 2 -blown microcellular non-isocyanate polyurethane (NIPU) foams: from bio- and CO 2 -sourced monomers to potentially thermal insulating materials, Green Chem. 18 (2016) 2206–2215, https://doi.org/10.1039/C5GC02723C.

[27] T. Dong, E. Dheressa, M. Wiatrowski, A.P. Pereira, A. Zeller, L.M.L. Laurens, P. T. Pienkos, Assessment of plant and microalgal oil-derived nonisocyanate polyurethane products for potential commercialization, ACS Sustain. Chem. Eng. 9 (2021) 12858–12869, https://doi.org/10.1021/acssuschemeng.1c03653.

[28] A. Cornille, S. Dworakowska, D. Bogdal, B. Boutevin, S. Caillol, A new way of creating cellular polyurethane materials: NIPU foams, Eur. Polym. J. 66 (2015) 129–138, https://doi.org/10.1016/j.eurpolymj.2015.01.034.

[29] A. Cornille, C. Guillet, S. Benyahya, C. Negrell, B. Boutevin, S. Caillol, Room temperature flexible isocyanate-free polyurethane foams, Eur. Polym. J. 84 (2016) 873–888, https://doi.org/10.1016/j.eurpolymj.2016.05.032.

[30] G. Coste, D. Berne, V. Ladmiral, C. Negrell, S. Caillol, Non-isocyanate polyurethane foams based on six-membered cyclic carbonates, Eur. Polym. J. 176 (2022) 111392, https://doi.org/10.1016/j.eurpolymj.2022.111392.

[31] N.S. Purwanto, Y. Chen, T. Wang, J.M. Torkelson, Rapidly synthesized, self- blowing, non-isocyanate polyurethane network foams with reprocessing to bulk networks via hydroxyurethane dynamic chemistry, Polymer (Guildf) 272 (2023) 125858, https://doi.org/10.1016/j.polymer.2023.125858.

[32] N.S. Purwanto, Y. Chen, J.M. Torkelson, Reprocessable, bio-based, self-blowing non-isocyanate polyurethane network foams from cashew nutshell liquid, ACS Appl. Polym. Mater. 5 (2023) 6651–6661, https://doi.org/10.1021/ acsapm.3c01196.

[33] F. Monie, B. Grignard, J. Thomassin, R. Mereau, T. Tassaing, C. Jerome, C. Detrembleur, Chemo- and regioselective additions of nucleophiles to cyclic carbonates for the preparation of self-blowing non-isocyanate polyurethane foams, Angew. Chem. Int. Ed. 59 (2020) 17033–17041, https://doi.org/10.1002/ anie.202006267.

[34] M. Bourguignon, B. Grignard, C. Detrembleur, Water-induced self-blown non- isocyanate polyurethane foams, Angew. Chem. Int. Ed. 61 (2022) e202213422, https://doi.org/10.1002/anie.202213422.

[35] M. Bourguignon, B. Grignard, C. Detrembleur, Cascade exotherms for rapidly producing hybrid nonisocyanate polyurethane foams from room temperature formulations, J. Am. Chem. Soc. 146 (2024) 988–1000, https://doi.org/10.1021/ jacs.3c11637.

[36] F. Monie, B. Grignard, C. Detrembleur, Divergent aminolysis approach for constructing recyclable self-blown nonisocyanate polyurethane foams, ACS Macro Lett. 11 (2022) 236–242, https://doi.org/10.1021/acsmacrolett.1c00793.

[37] M. Makarov, M. Bourguignon, B. Grignard, C. Detrembleur, Advancing non- isocyanate polyurethane foams: exo -vinylene cyclic carbonate–amine chemistry enabling room-temperature reactivity and fast self-blowing, Macromolecules 58 (2025) 1673–1685, https://doi.org/10.1021/acs.macromol.4c02894.

[38] M. Bourguignon, B. Grignard, C. Detrembleur, Fast, catalyst-free room temperature production of isocyanate-free polyurethane foams using aromatic thiols, Polym. Chem. 16 (2025) 192–203, https://doi.org/10.1039/D4PY00971A.

[39] C. Detrembleur, B. Grignard, M. Bourguignon, Self-blowing isocyanate-free polyurethane foams, WO 2023/104362, 2023.

[40] Y. Chen, N.S. Purwanto, B. Chen, T. Wang, S. Kim, Y.-W. Huang, W.R. Dichtel, J. M. Torkelson, Biobased, catalyst-free non-isocyanate polythiourethane foams: Highly dynamic nature affords fast reprocessability, extrudability and refoamability, Chem. Eng. J. 496 (2024) 154035, https://doi.org/10.1016/j. cej.2024.154035.

[41] N.S. Purwanto, Y. Chen, J.M. Torkelson, Biobased, reprocessable, self-blown non- isocyanate polyurethane foams: Influence of blowing agent structure and functionality, Eur. Polym. J. 206 (2024) 112775, https://doi.org/10.1016/J.EURPOLYMJ.2024.112775.

[42] T. Wang, H. Deng, H. Zeng, J. Shen, F. Xie, C. Zhang, Self-blowing non-isocyanate polyurethane foams from cyclic carbonate linseed oil, ACS Sustainable Resour Manage 1 (2024) 462–470, https://doi.org/10.1021/ACSSUSRESMGT.3C00103.

[43] J. Sternberg, S. Pilla, Materials for the biorefinery: high bio-content, shape memory Kraft lignin-derived non-isocyanate polyurethane foams using a non-toxic protocol, Green Chem. 22 (2020) 6922–6935, https://doi.org/10.1039/D0GC01659D.

[44] M. Ghasemlou, F. Daver, E.P. Ivanova, B. Adhikari, Bio-based routes to synthesize cyclic carbonates and polyamines precursors of non-isocyanate polyurethanes: A review, Eur. Polym. J. 118 (2019) 668–684, https://doi.org/10.1016/j. eurpolymj.2019.06.032.

[45] Trojanowska, F. Monie, G. Perotto, A. Athanassiou, B. Grignard, E. Grau, T. Vidil, H. Cramail, C. Detrembleur, Valorization of waste biomass for the fabrication of isocyanate-free polyurethane foams, Green Chem. 26 (2024) 8383–8394, https://doi.org/10.1039/D4GC01547A.

[46] C. Bakkali-Hassani, D. Berne, P. Bron, L. Irusta, H. Sardon, V. Ladmiral, S. Caillol, Polyhydroxyurethane covalent adaptable networks: looking for suitable catalysts, Polym. Chem. 14 (2023) 3610–3620, https://doi.org/10.1039/D3PY00579H.

[47] X. Chen, L. Li, K. Jin, J.M. Torkelson, Reprocessable polyhydroxyurethane networks exhibiting full property recovery and concurrent associative and dissociative dynamic chemistry: Via transcarbamoylation and reversible cyclic carbonate aminolysis, Polym. Chem. 8 (2017) 6349–6355, https://doi.org/ 10.1039/c7py01160a.

[48] T. Wang, Y. Chen, B. Chen, M.J. Suazo, N.S. Purwanto, J.M. Torkelson, Reprocessable, self-healing, and creep-resistant covalent adaptable network made from chain-growth monomers with dynamic covalent thionourethane and disulfide cross-links, ACS Macro. Lett. 13 (2024) 1147–1155, https://doi.org/10.1021/ acsmacrolett.4c00391.

[49] Y. Chen, N. Mielke, N.S. Purwanto, B. Chen, C.D. Malliakas, J.M. Torkelson, Non- isocyanate polythiourethane network from biowaste: achieving circularity via multidimensional chemical recycling with valuable small-molecule recovery and reprocessability by understanding the dynamic chemistry, Macromolecules 57 (2024) 490–502, https://doi.org/10.1021/acs.macromol.3c01941.

[50] C. Pronoitis, M. Hakkarainen, K. Odelius, Structurally diverse and recyclable isocyanate-free polyurethane networks from CO2-derived cyclic carbonates, ACS Sustain Chem Eng 10 (2022) 2522–2531, https://doi.org/10.1021/ acssuschemeng.1c08530.

[51] D.J. Fortman, R.L. Snyder, D.T. Sheppard, W.R. Dichtel, Rapidly reprocessable cross-linked polyhydroxyurethanes based on disulfide exchange, ACS Macro Lett. 7 (2018) 1226–1231, https://doi.org/10.1021/acsmacrolett.8b00667.

[52] L. Li, X. Chen, J.M. Torkelson, Covalent adaptive networks for enhanced adhesion: exploiting disulfide dynamic chemistry and annealing during application, ACS Appl. Polym. Mater. 2 (2020) 4658–4665, https://doi.org/10.1021/ acsapm.0c00720.

[53] Y. Chen, B. Chen, J.M. Torkelson, Biobased, reprocessable non-isocyanate polythiourethane networks with thionourethane and disulfide cross-links: comparison with polyhydroxyurethane network analogues, Macromolecules 56 (2023) 3687–3702, https://doi.org/10.1021/acs.macromol.3c00220.

[54] W.E. Savige, J.A. Maclaren, Oxidation of disulfides, with special reference to cystine, in: N. Kharasch, C.Y. Meyers (Eds.), The Chemistry of Organic Sulfur Compounds, Elsevier, Amsterdam, 1966, pp. 367–402.

[55] S. Panchireddy, J.M. Thomassin, B. Grignard, C. Damblon, A. Tatton, C. Jerome, C. Detrembleur, Reinforced poly(hydroxyurethane) thermosets as high performance adhesives for aluminum substrates, Polym. Chem. 8 (2017) 5897–5909, https://doi.org/10.1039/c7py01209h.

[56] I.S. Alferiev, J.M. Connolly, R.J. Levy, A novel mercapto-bisphosphonate as an efficient anticalcification agent for bioprosthetic tissues, J. Organomet. Chem. 690 (2005) 2543–2547, https://doi.org/10.1016/j.jorganchem.2004.10.011.

[57] G.G. Jayson, T.C. Owen, A.C. Wilbraham, The radiation chemistry of cystamine sulphate, J. Chem. Soc. B (1967) 944, https://doi.org/10.1039/j29670000944.

[58] D.J. Fortman, J.P. Brutman, M.A. Hillmyer, W.R. Dichtel, Structural effects on the reprocessability and stress relaxation of crosslinked polyhydroxyurethanes, J. Appl. Polym. Sci. 134 (2017) 44984, https://doi.org/10.1002/app.44984.

[59] F. Monie, T. Vidil, E. Grau, B. Grignard, C. Detrembleur, H. Cramail, The Multifaceted role of water as an accelerator for the preparation of isocyanate-free polyurethane thermosets, Macromolecules 57 (2024) 8877–8888, https://doi.org/ 10.1021/acs.macromol.4c01672.

[60] F. Van Lijsebetten, K. De Bruycker, E. Van Ruymbeke, J.M. Winne, F.E. Du Prez, Characterising different molecular landscapes in dynamic covalent networks, Chem. Sci. 13 (2022) 12865–12875, https://doi.org/10.1039/D2SC05528G.

[61] G. Deng, F. Li, H. Yu, F. Liu, C. Liu, W. Sun, H. Jiang, Y. Chen, Dynamic hydrogels with an environmental adaptive self-healing ability and dual responsive Sol-Gel transitions, ACS Macro Lett. 1 (2012) 275–279, https://doi.org/10.1021/ mz200195n.

[62] C. Luo, Z. Lei, Y. Mao, X. Shi, W. Zhang, K. Yu, Chemomechanics in the moisture- induced malleability of polyimine-based covalent adaptable networks, Macromolecules 51 (2018) 9825–9838, https://doi.org/10.1021/acs.macromol.8b02046.

[63] P. Taynton, K. Yu, R.K. Shoemaker, Y. Jin, H.J. Qi, W. Zhang, Heat- or water-driven malleability in a highly recyclable covalent network polymer, Adv. Mater. 26 (2014) 3938–3942, https://doi.org/10.1002/adma.201400317.

[64] P. Sen Choong, N.X. Chong, E.K. Wai Tam, A.M. Seayad, J. Seayad, S. Jana, Biobased nonisocyanate polyurethanes as recyclable and intrinsic self-healing coating with triple healing sites, ACS Macro Lett. 10 (2021) 635–641, https://doi. org/10.1021/acsmacrolett.1c00163.

[65] S. Panchireddy, B. Grignard, J.M. Thomassin, C. Jerome, C. Detrembleur, Bio- based poly(hydroxyurethane) glues for metal substrates, Polym. Chem. 9 (2018) 2650–2659, https://doi.org/10.1039/c8py00281a.

[66] S. Panchireddy, B. Grignard, J.-M. Thomassin, C. Jerome, C. Detrembleur, Catechol containing polyhydroxyurethanes as high-performance coatings and adhesives, ACS Sustain. Chem. Eng. 6 (2018) 14936–14944, https://doi.org/10.1021/ acssuschemeng.8b03429.

[67] A. Gomez-Lopez, S. Panchireddy, B. Grignard, I. Calvo, C. Jerome, C. Detrembleur, H. Sardon, Poly(hydroxyurethane) adhesives and coatings: state-of-the-art and future directions, ACS Sustain. Chem. Eng. 9 (2021) 9541–9562, https://doi.org/ 10.1021/acssuschemeng.1c02558.

[68] C.R. Matos-Perez, J.D. White, J.J. Wilker, Polymer composition and substrate ´ influences on the adhesive bonding of a biomimetic, cross-linking polymer, J. Am. Chem. Soc. 134 (2012) 9498–9505, https://doi.org/10.1021/ja303369p.

[69] B.T. Michal, E.J. Spencer, S.J. Rowan, Stimuli-responsive reversible two-level adhesion from a structurally dynamic shape-memory polymer, ACS Appl. Mater. Interfaces 8 (2016) 11041–11049, https://doi.org/10.1021/acsami.6b01251.

[70] J. Canadell, H. Goossens, B. Klumperman, Self-healing materials based on disulfide links, Macromolecules 44 (2011) 2536–2541, https://doi.org/10.1021/ ma2001492.

[71] L. Imbernon, E.K. Oikonomou, S. Norvez, L. Leibler, Chemically crosslinked yet reprocessable epoxidized natural rubber via thermo-activated disulfide rearrangements, Polym. Chem. 6 (2015) 4271–4278, https://doi.org/10.1039/ C5PY00459D.

[72] I. Azcune, I. Odriozola, Aromatic disulfide crosslinks in polymer systems: Self- healing, reprocessability, recyclability and more, Eur. Polym. J. 84 (2016) 147–160, https://doi.org/10.1016/j.eurpolymj.2016.09.023.

[73] P. Verdugo, D. Santiago, S. De la Flor, A. Serra, A biobased epoxy vitrimer with ` dual relaxation mechanism: A promising material for renewable, reusable, and recyclable adhesives and composites, ACS Sustain. Chem. Eng. 12 (2024) 5965–5978, https://doi.org/10.1021/acssuschemeng.4c00205.

[74] S. Ebnesajjad, A.H. Landrock, Characteristics of Adhesive Materials, in: S. Ebnesajjad, A. H. Landrock (Eds.), Adhesives Technology Handbook, Elsevier, Amsterdam, 2015: pp. 84–159. https://doi.org/10.1016/B978-0-323-35595- 7.00005-X.

[75] F. Van Lijsebetten, T. Debsharma, J.M. Winne, F.E. Du Prez, A highly dynamic covalent polymer network without creep: mission impossible? Angew. Chem. Int. Ed. 61 (2022) e202210405 https://doi.org/10.1002/anie.202210405.

[76] M.A. Bin Rusayyis, J.M. Torkelson, Reprocessable covalent adaptable networks with excellent elevated-temperature creep resistance: facilitation by dynamic, dissociative bis(hindered amino) disulfide bonds, Polym. Chem. 12 (2021) 2760–2771, https://doi.org/10.1039/D1PY00187F.

[77] R. Yi, C. Chen, Y. Li, H. Peng, H. Zhang, X. Ren, The bonding between glass and metal, Int. J. Adv. Manuf. Technol. 111 (2020) 963–983, https://doi.org/10.1007/ s00170-020-06018-x.

[78] M. Overend, Q. Jin, J. Watson, The selection and performance of adhesives for a steel–glass connection, Int. J. Adhes Adhes 31 (2011) 587–597, https://doi.org/ 10.1016/j.ijadhadh.2011.06.001.

[79] A.M. Pereira, J.M. Ferreira, F.V. Antunes, P.J. Bartolo, Analysis of manufacturing ´ parameters on the shear strength of aluminium adhesive single-lap joints, J Mater Process Technol 210 (2010) 610–617, https://doi.org/10.1016/j.jmatprotec.2009.11.006.

[80] G. Critchlow, Surface Treatments, in: L.F.M. da Silva, A. Ochsner, R.D. Adams ¨(Eds)., Handbook of Adhesion Technology, in Springer Berlin Heidelberg, Berlin, Heidelberg, 2011: pp. 119-146. https://doi.org/10.1007/978-3-642-01169-6.

[81] C. Bao, Y. Yin, Y. Ding, J. Liu, Y. Xu, R. Miao, Z. Liu, B. Duan, Y. Qin, Z. Xin, Chemically recyclable supramolecular thermosets toward strong and reusable hot- melt adhesives, Macromolecules 56 (2023) 6633–6643, https://pubs.acs.org/doi/10.1021/acs.macromol.3c01063.

[82] Y. Tian, X. Huang, Y. Cheng, Y. Niu, J. Ma, Y. Zhao, X. Kou, Q. Ke, Applications of adhesives in textiles: A review, Eur. Polym. J. 167 (2022) 111089, https://doi.org/10.1016/J.EURPOLYMJ.2022.111089.

[83] M.A. Rahman, C. Bowland, S. Ge, S.R. Acharya, S. Kim, V.R. Cooper, X.C. Chen, S. Irle, A.P. Sokolov, A. Savara, T. Saito, Design of tough adhesive from commodity thermoplastics through dynamic crosslinking, Sci. Adv. 7 (2021) eabk2451, https://doi.org/10.1126/sciadv.abk2451.